JOURNAL OF GEOPHYSICAL RESEARCH, VOL. 99, NO. B11, PAGES 22,093–22,119, NOVEMBER 10, 1994

Thermal regime of the southern Basin and Range Province: 1. Heat flow data from Arizona and the Mojave Desert of California and Nevada

J. H. Sass,[1] Arthur H. Lachenbruch,[2] S. P. Galanis Jr.,[2] Paul Morgan,[3] S. S. Priest,[1] T. H. Moses Jr.,[2] and R. J. Munroe[2]

Abstract. With about 150 new heat flow values, more than 200 values of heat flow are now available from the crystalline terranes of southern California, the Basin and Range Province of Arizona, and Paleozoic sedimentary rocks of the southwestern Colorado Plateau (CP). Heat flow ranges from about 5 mW m^{-2} on the CP near Flagstaff, Arizona, to more than 150 mW m^{-2} in the crystalline rocks bordering the Salton Trough in SE California. The heat flow pattern within this region is complex, although it correlates with regional physiographic and tectonic features. Unlike the adjacent Sierra Nevada Batholith where heat flow is a linear function of near-surface radiogenic heat production, no statistically significant correlation exists between heat flow and heat production in the study area, possibly because of its complex tectonic history, involving lateral movement of basement terranes, and relatively young heat sources and sinks of different strengths, ages, and durations. Contemporary and Neogene extensional tectonism appears to be responsible for the very high heat flow (>100 mW m^{-2}) associated with the Salton Trough and its neighboring ranges, the Death Valley fault zone and its southward extension along the eastern boundary of the Mojave block, and zones of shallow depth (<10 km) to the Curie isotherm (as inferred from aeromagnetic data) in west central Arizona. Low (<60 mW m^{-2}) heat flow in the Peninsular Ranges and eastern Transverse Ranges of California may be caused by downward advection associated with subduction and compressional tectonics. Relatively low heat flow (67 ± 4 mW m^{-2}) is also associated with the main trend of metamorphic core complexes in Arizona, and the outcropping rocks in the core complexes have a low radioactive heat production (1.3 ± 0.3 μW m^{-3}) compared to the other crystalline rocks in the region (2.1 ± 0.2 μW m^{-3}).

Introduction

The states of Arizona and California and Nevada south of latitude 37° encompass a large number of tectonic regimes and many heat flow provinces, even on a large scale (Figure 1). Early regional studies recognized the thermal complexity of the Western U.S. Cordillera [*Roy et al.*, 1968b, 1972; *Blackwell*, 1969; *Sass et al.*, 1971b], and the data set has provided a basis for numerous interpretive studies [*Lachenbruch*, 1968a, 1970; *Roy et al.*, 1972; *Blackwell*, 1978; *Lachenbruch and Sass*, 1973, 1977, 1978, 1980, 1981; *Lachenbruch et al.*, 1985]. We have acquired about 150 new heat flow data in crystalline rocks of the region contained within the box in Figure 1, mainly from relatively shallow (100–250 m) wells drilled as part of the U.S. Geological Survey (USGS) Earthquake Prediction, Geothermal Resources, Geologic Framework and Deep Continental Studies programs. A few additional holes were drilled at locations critical to the USGS Pacific to Arizona Crustal Experiment (PACE) transect [see *Sass et al.*, 1988a; *Howard et al.*, 1990]. Results from some parts of the region have been published and interpreted. In particular, *De Rito et al.* [1989] have completed a heat flow reconnaissance of the Ventura Basin, *Saltus et al.* [1988] and *Saltus and Lachenbruch* [1991] have discussed the thermal regime of the southern Sierra Nevada, and *Lachenbruch et al.* [1985] have presented most of the data from southern California and westernmost Arizona in the context of the Salton Trough. The geothermal setting of the Cajon Pass scientific research well was described by *Lachenbruch et al.* [1986a, b] and by *Sass et al.* [1986]; heat flow at Cajon Pass and its implications for the "stress/heat flow paradox" are the subject of papers by *Lachenbruch and Sass* [1988], *Sass et al.* [1992], and *Lachenbruch and Sass* [1992]. *Sass et al.* [1981b, 1982] presented new data from the Arizona Basin and Range and Colorado Plateau, respectively, and *Sass and Lachenbruch* [1987] gave a preliminary presentation of data from the entire region. Earlier data and their sources were reviewed by *Sass et al.* [1981a], *Morgan and Gosnold* [1989], *Blackwell et al.* [1991], and *Blackwell and Steele* [1992].

In this study, we characterize the thermal regime of the entire southern Basin and Range Province by combining the new data with previously published results and placing them in the context of the surrounding thermotectonic provinces including the northern Basin and Range (or Great Basin), southern Sierra Nevada, Peninsular Ranges, Transverse Ranges,

[1]U.S. Geological Survey, Flagstaff, Arizona.
[2]U.S. Geological Survey, Menlo Park, California.
[3]Department of Geology, Northern Arizona University, Flagstaff.

Paper number 94JB01891.
0148-0227/94/94JB-01891$05.00

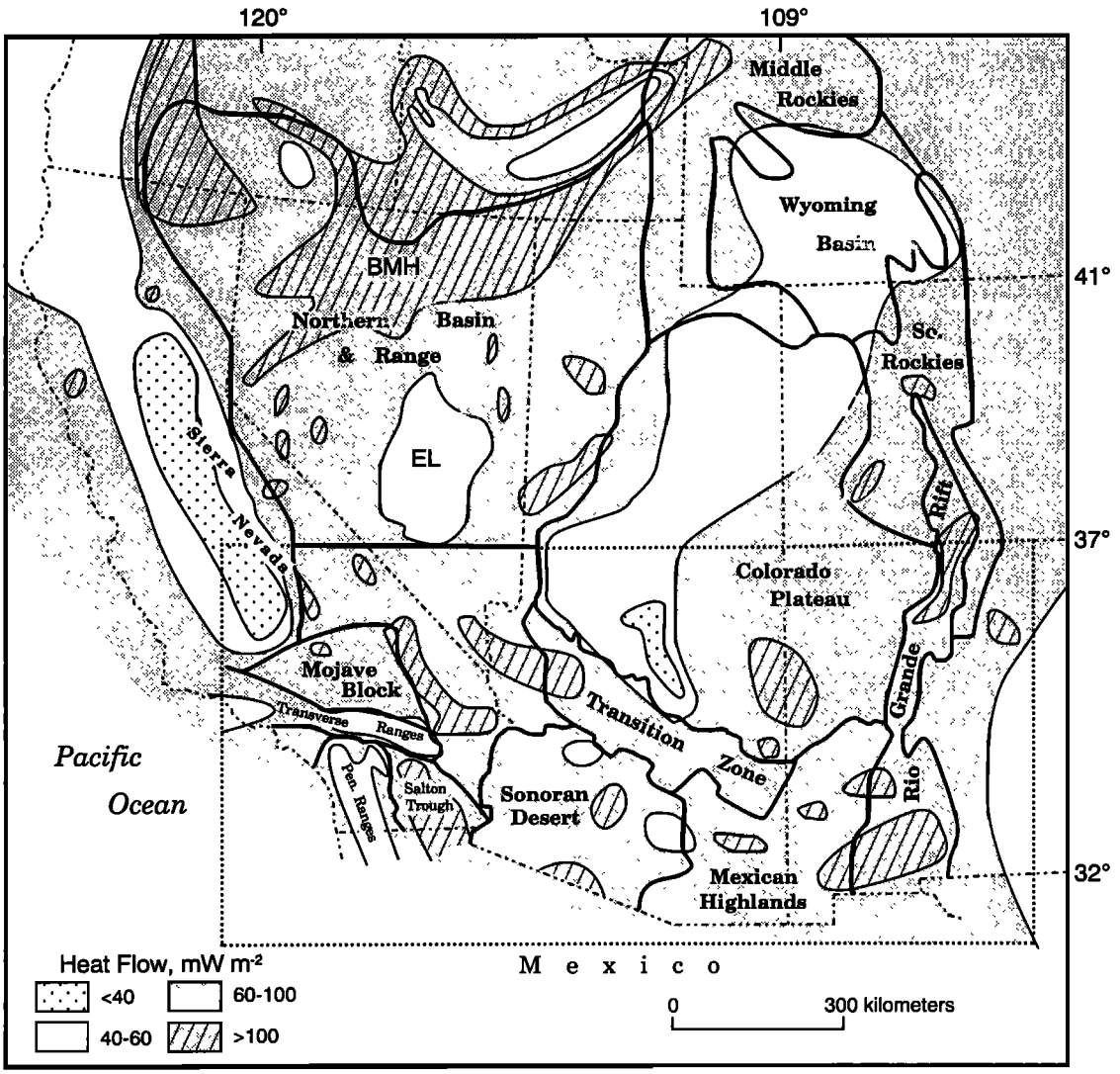

Figure 1. Generalized map of physiography and heat flow from the southwestern United States (modified from *Sass et al.*, [1981a]). Box (dotted lines) encloses the area considered in this study (Figures 3–6).

Salton Trough, and Colorado Plateau (Figure 1). We then discuss the relationship of the thermal patterns to the distribution of near-surface radioactivity in crystalline rocks. In the sections that follow, we describe our techniques and procedures, present the data, and provide a generalized discussion of the observed heat flow pattern in terms of the major tectonic features, regional hydrology, and Cenozoic thermal history of the region.

Site Selection and Drilling

Most of the ~150 new heat flow data presented here are based on measurements in wells drilled specifically for heat flow. They are all relatively shallow (100–250 m) but are located on sites where topographic and hydrologic disturbances are likely to be minimal. Several criteria were applied to the selection of sites to maximize the probability of obtaining a reliable heat flow datum at a depth that could be drilled easily by a truck-mounted rig in a few days. First and foremost, the wells were sited on intrusive and metamorphic crystalline rock whose relative homogeneity facilitates sampling for thermal conductivity and radioelement abundances and in which near-surface radiogenic heat production provides information on the upper crustal component of heat flow. Second, the wells were located at least one hill height from the nearest topographic features, on local topographic lows. This generally results in topographic corrections of less than 10% [see *Lachenbruch*, 1968b]. Third, they were located away from springs or other manifestations of nearby vertical water movement to minimize the probability of hydrologic disturbances to the temperature profiles [see *Bredehoeft and Papadopulos*, 1965; *Lachenbruch and Sass*, 1977].

In scientific drilling, the ideal situation is one in which a continuous core is obtained, resulting in an unambiguous record of the rocks penetrated, with whole rock samples upon which to measure critical parameters and to calibrate downhole measurements. In some applications, the cost of continuous coring is competitive with percussion-type drilling, but in this project, using the technology available to us at the time, continuous coring was prohibitively expensive. Even obtaining one 1.5-m-long core virtually doubled the

Table 1. A Comparison Between Thermal Conductivity Measured on Core and That From Drill Cuttings for Boreholes in the Mojave and Sonoran Deserts

Well Designation	Thermal Conductivity, W m^{-1} K^{-1}				Scatter*	
	Core	Adjacent Cuttings	Number of Samples	Cuttings Average	S.D.	95% C.I.
PCK	3.36	3.48	10	3.39	0.29	0.18
DAV	3.36	3.42	9	3.51	0.27	0.18
FPK	2.64	2.35	26	2.39	0.19	0.08
DCH	2.50	2.80	9	2.93	0.21	0.14
KNG	4.12†	3.31	10	3.56	0.27	0.18
	3.53‡					
RGA	2.42	2.55	12	2.45	0.19	0.12
RGC	2.80	2.99	9	2.82	0.27	0.18
RGE	3.12	2.88	8	2.99	0.27	0.20
RGF	3.60	2.87	8	2.66	0.31	0.22
RGG	1.88	1.81	8	1.86	0.22	0.16

*S.D., standard deviation; 95% C.I., 95% confidence interval.
†Heat conducted parallel to foliation.
‡Heat conducted perpendicular to foliation.

cost per hole of drilling and completion. The crystalline rocks of the Mojave and Sonoran Deserts provided an ideal medium for drilling holes up to 500 m deep using a downhole hammer with bits having tungsten carbide inserts. Typical penetration rates were 10 m/h or more so that a 100-m hole could be drilled and completed in $1\frac{1}{2}$ to 2 days and a 200-m hole in 3–4 days. Rigging up and obtaining a 1.5-m core usually took at least an extra day and more often than not, wore out a diamond core bit. Thus, by far the most cost effective means of hole-production was the downhole hammer method.

Even where the holes have been carefully sited away from springs and seeps, vertical water movement in the borehole can result in significant errors to heat flow estimates. The upper 200–300 m of crystalline terranes tends to be pervasively fractured and weathered. Very small vertical head differences between previously unconnected fracture systems can result in vertical flow in the hole with particle velocities sufficiently high to overwhelm the conductive geothermal flux. All holes were cased with relatively inexpensive 32 mm ID steel or plastic pipe to maintain access for temperature measurements. To ensure against vertical water movement in the lower part of the annulus, we sealed it with a Portland cement-bentonite grout. This "ten sack" grout [*Moses and Sass*, 1979] was a trade-off between mixing enough grout to fill the entire annulus and the quantity of material that could be hauled to the site in a 3/4-ton pickup truck. Depending on the hole diameter (nominally in the range 10–20 cm), this mixture would fill between 20 and 100 m of the annulus.

After completion, each hole was logged several times over a period of 1–2 years (see the appendix), a period sufficient to monitor the decay of drilling and grouting transients and to establish an equilibrium temperature profile. At the conclusion of the process, the casing was cut off below ground level, the hole was plugged, and the drill pad restored to as natural a state as possible.

Measurement and Data Reduction Techniques

Heat flow is the product of vertical temperature gradient and thermal conductivity. At a given depth z, the heat flow q is

Table 2. A Comparison Between Total Radiogenic Heat Production From Core and That From Cuttings for Core Holes in the Mojave and Sonoran Deserts

Well Designation	Heat Production, μW m^{-3}				Scatter*	
	Core	Adjacent Cuttings	Number of Samples	Cuttings Average	S.D.	95% C.I.
PCK	2.34	2.01	5	2.43	0.49	0.44
VAL	0.87	1.08	4	1.08	0.15	0.16
DAV	1.23	1.53	10	3.17	0.84	0.54
FPK	1.01	1.21	6	0.83	0.12	0.10
	0.92	1.16				
DCH	6.22	5.32	4	5.02	0.33	0.32
KNG	1.76	3.01	6	3.52	1.84	1.50
	1.76					
RGA	0.63	0.72	7	1.61	0.57	0.44
RGB	1.01	0.95	6	1.03	0.11	0.10
RGC	1.05	0.94	5	0.84	0.06	0.04
RGE	0.91	1.67	4	1.55	0.56	0.56
RGF	0.70	1.81	5	1.60	0.54	0.44
RGG	0.54	0.65	5	0.64	0.04	0.04

*S.D., standard deviation; 95% C.I., 95% confidence interval.

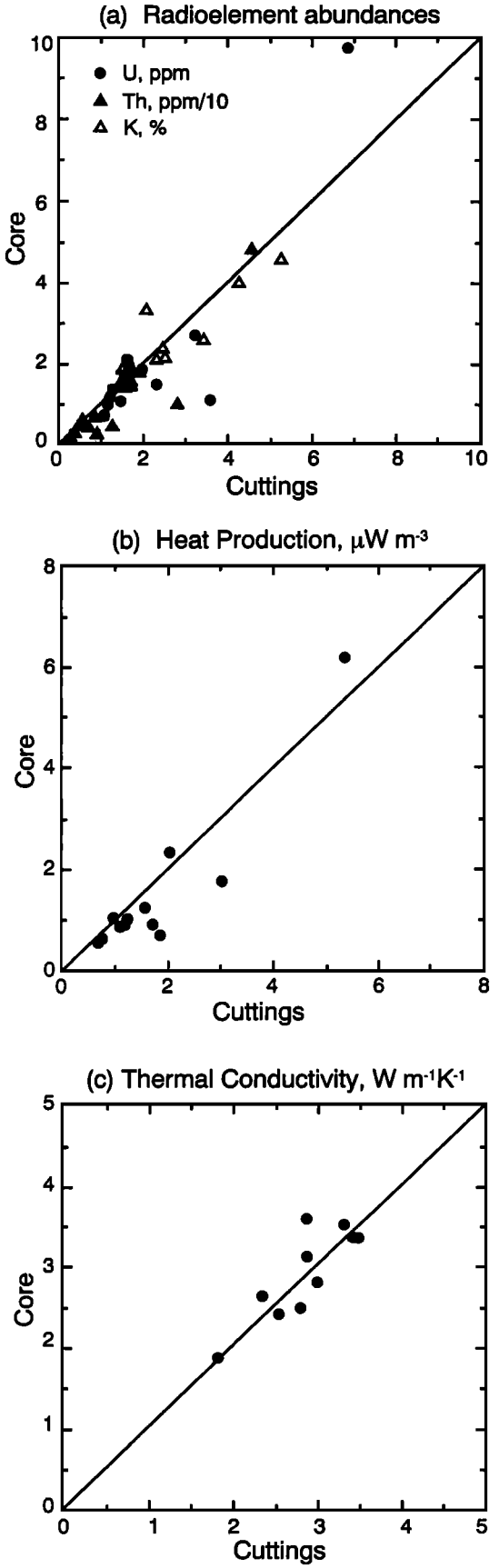

Figure 2. Comparisons of heat production and thermal conductivity measurements on core and cuttings (see also Tables 1 and 2): (a) radioelement abundances; (b) radiogenic heat production; and (c) thermal conductivity.

$$q(z) = \frac{-\partial T}{\partial z}\lambda(z) \quad (1)$$

where T is temperature and λ is thermal conductivity. Temperature gradients are obtained from high-resolution (1 mK) closely spaced (0.3–3 m) temperature logs [*Blackwell and Spafford*, 1987; *Beck and Balling*, 1988]. Thermal conductivity is measured in the laboratory on solid samples of core or outcrops, or on drill cuttings, using a steady state divided-bar type apparatus or a transient line source [*Beck*, 1988; *Decker et al.*, 1988; *Sass et al.*, 1971a, 1984a, b, c]. The methods of combining thermal conductivity and temperature data are reviewed by *Powell et al.* [1988]. In this study, all heat flow values were calculated over one or more intervals by combining the least squares temperature gradient (Γ, °C km^{-1} or mK m^{-1}) with the harmonic mean thermal conductivity ($\langle\lambda\rangle$, W m^{-1} K^{-1}). As stated above in the discussion of drilling procedures, dedicated holes were sited so as to minimize topographic effects; however, in the relatively few instances (about a dozen) where application of the simple "plane slope" models of *Lachenbruch* [1968b] indicated a sizeable (≳5%) correction, a three-dimensional *Birch* [1950] type correction or a two-dimensional Lees Hill correction [*Jaeger and Sass*, 1963] was performed as appropriate.

The upper crustal contribution of radiogenic heat to the observed heat flow generally is a substantial fraction of the total. Thus, in crystalline terranes, measurement of the near-surface radiogenic heat production (A_0) should allow a more complete interpretation of heat flow than would otherwise be possible. For all dedicated drill holes and all "scrounged" holes from which sufficient material was available, we measured A_0 on 5 to 10 ~1 kg samples distributed along the length of the hole. Abundances of U, Th, and K were measured using gamma ray spectrometry [*Wollenberg*, 1977; *Rybach*, 1988].

The primary disadvantage of the rotary percussion drilling method for scientific studies is the type of samples obtained; drill cuttings ranging in size from a fine powder to thumbnail-sized fragments. The critical question is whether the drill cuttings are sufficiently representative to allow accurate characterization of thermal conductivity and radiogenic heat production. To test this, we obtained spot cores near or at the bottom of 12 holes. The appropriate measurements were made both on plugs (conductivity) or crushed core (radiogenic heat production) and adjacent cuttings samples. The results of the comparisons are summarized in Tables 1 and 2 and in Figure 2. For two of the cores (RGB and VAL), there was insufficient unbroken material to prepare disks for determinations of thermal conductivity, so that only 10 conductivity comparisons could be made (Table 1 and Figure 2c). From the comparisons (Tables 1 and 2 and Figure 2), we can make the following observations: (1) In the majority of cases, the results for core and cuttings are within 15% of each other (the combined accuracy of the two determinations). (2) There is a tendency for both uranium and thorium to be enriched in cuttings relative to crushed core (Figure 2a), particularly at low abundances. (3) Total heat production (Figure 2b) averages about 5% higher for cuttings than core, whereas thermal conductivity averages about 2% lower (Figure 2c).

The results for thermal conductivity are satisfactory, particularly since we were using adjacent cuttings samples

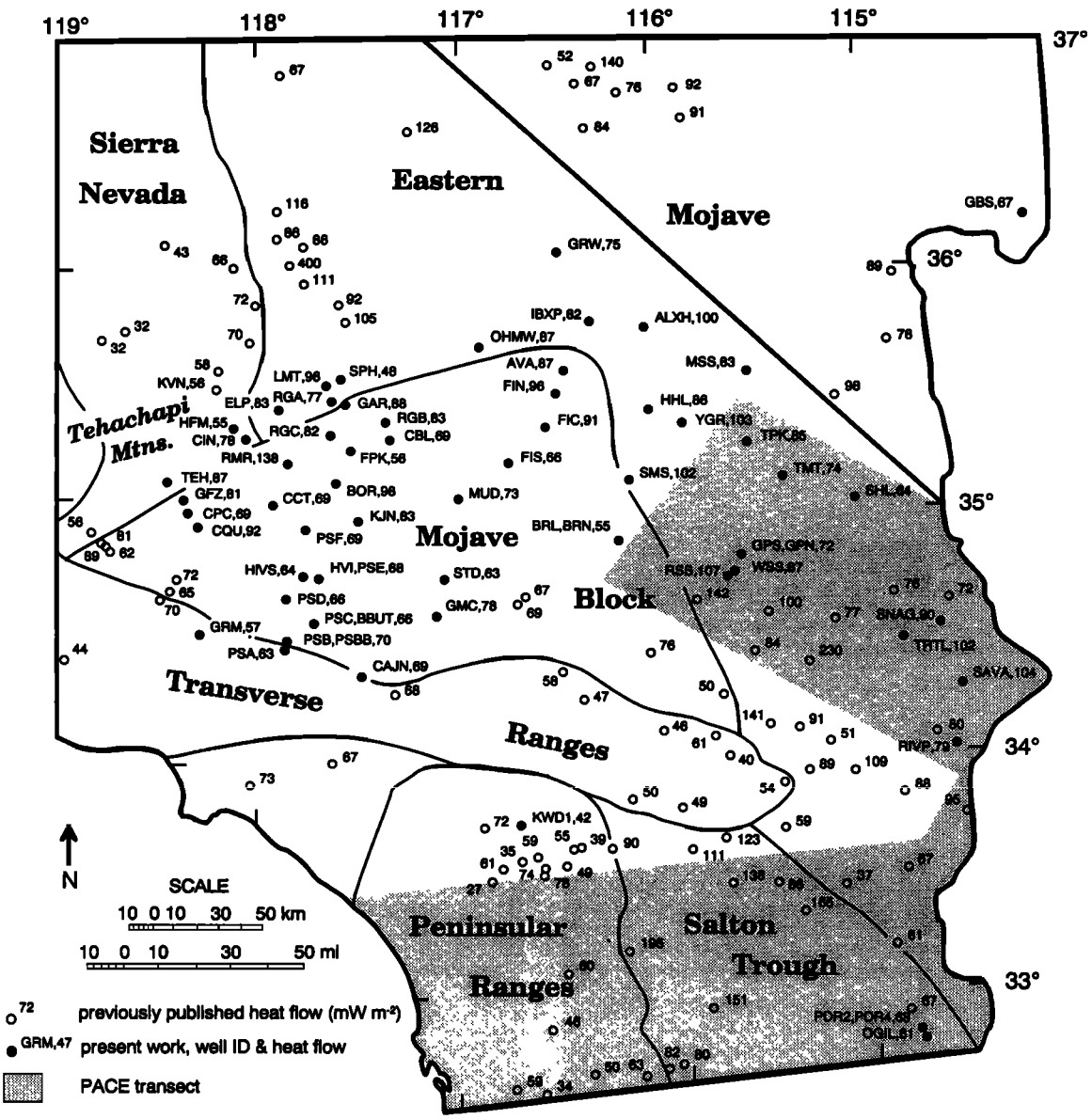

Figure 3. Map of southernmost California and Nevada showing major physiographic/tectonic provinces, locations of heat flow determinations and heat flow values. Previously published values include those of *Roy et al.* [1968b], *Henyey* [1968], *Henyey and Wasserburg* [1971], *Sass et al.* [1971b], *Lee* [1983], and *Lachenbruch et al.* [1985]. Shaded area encloses the various geologic and geophysical transects that compose the Pacific to Arizona Crustal Experiment (PACE).

rather than cuttings obtained over the cored interval. The latter interval was usually the bottom of the hole, and the very small amount of very fine cuttings obtained while coring was not a suitable sample. One core sample (KNG, Table 1) exhibited a distinct gneissic texture. From measurements on disks cut parallel and perpendicular to the foliation, the apparent anisotropy is about 1.17. For anisotropic rocks (assuming horizontal foliation), measurements on an aggregate of chips will tend to overestimate the vertical conductivity [see *Sass et al.*, 1992]. Judging from the other holes involved in the comparisons and from outcrops at other drill sites, anisotropy is not a serious problem in this study.

Uranium and thorium are commonly concentrated in small particles on grain boundaries and are likely to be mobilized by the percussion process. The apparent enrichment of cuttings relative to core at low abundances of U and Th (Figure 2a) may well be caused by a gravity separation of the heavier U and Th compounds in the flow line. For this project, the sample was obtained by placing an ordinary kitchen sieve in the ditch carrying water and cuttings. If the heavier particles settled to the bottom of the ditch, some enrichment would result. From our observations (Figures 2a and 2b), we conclude that most determinations of heat production and average values will be satisfactory but that we cannot place a lot of emphasis on any individual determination, particularly for low abundances. This is in contrast to the situations where the cuttings sample is obtained from a "shaker table" or similar sieving device. Severe depletion of uranium and thorium usually occurs during this process [see *Lachenbruch and Bunker*, 1971; *Sass et al.*, 1992].

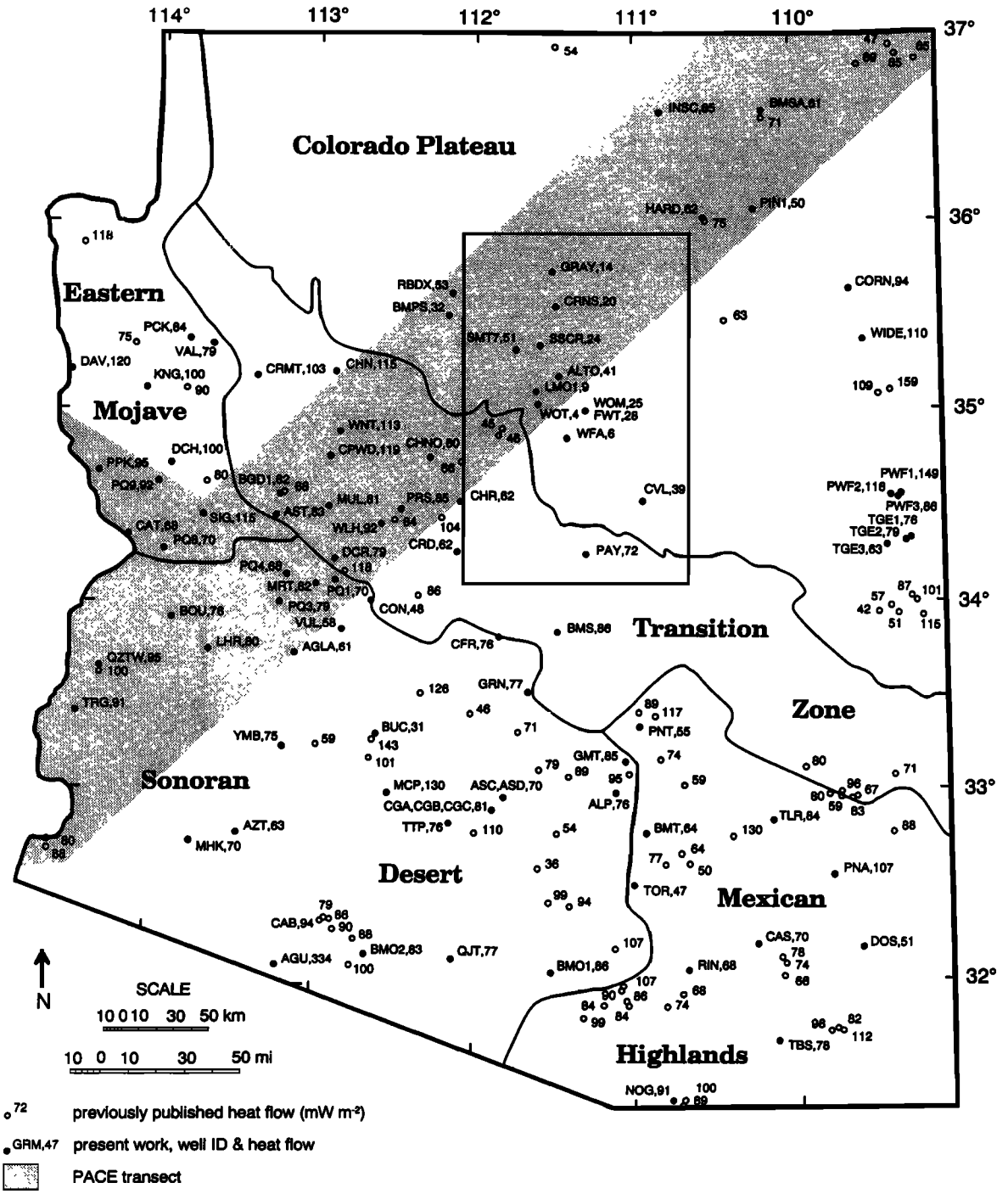

Figure 4. Map of Arizona showing major physiographic/tectonic provinces, locations of heat flow determinations and heat flow values. Previously published values include those of *Roy et al.* [1968b], *Wcrren et al.* [1969], *Sass et al.* [1971b], *Shearer and Reiter* [1981], and *Sass et al.* [1981b, 1982]. Inner rectangle defines the area of Figure 7. Shaded area indicates locus of PACE transect.

Results

Heat Flow

Heat flow data are plotted on the maps of Figures 3 and 4. Also shown as a shaded area on these figures is the locus of the PACE transect including seismic lines, gravity, magnetic and magnetotelluric traverses, and geologic strip maps. Temperature profiles are presented in the appendix. The principal elements of each heat flow calculation are summarized in Tables 3–8. Where details of heat flow calculations have been published elsewhere, an abridged summary is given (Tables 9 and 10). It was convenient to group heat flow values within recognized physiographic-tectonic provinces for the purposes of cross-referencing tables and temperature profiles. Most of the open circles in Figure 3 represent sites discussed by *Lachenbruch et al.* [1985] to provide a context for thermal models of the Salton Trough. They also include

Table 3. Thermal Data for Crystalline Rocks of the Mojave Block

Well Designation	Latitude N	Longitude W	Elevation, m	Depth Range, m	Gradient,* °C km^{-1}		Thermal Conductivity,† W m^{-1} K^{-1}		Heat Flow, mW m^{-2}	Heat Production, μW m^{-3}
					Γ_m	Γ_c	N	⟨K⟩		
KJN	34°58.4′	117°29.7′	802	30–101	29.51 ± 0.05	29.5	16	2.81 ± 0.05	83 ± 2	1.3
CPC	35°00.8′	118°20.6′	1183	38–154	22.69 ± 0.04	21.7	10	3.17 ± 0.04	69 ± 2	1.7
CCT	35°02.4′	117°55.0′	757	61–152	26.12 ± 0.05	26.1	8	2.64 ± 0.04	69 ± 1	1.1
GFZ	35°03.4′	118°21.7′	1347	76–154	28.55 ± 0.01	28.9	7	2.79 ± 0.04	81 ± 2	1.9
MUD	35°03.6′	117°00.0′	1244	60–102	26.36 ± 0.13	26.4	5	2.77 ± 0.04	73 ± 1	2.6
BOR	35°07.7′	117°35.9′	870	30–53	43.6 ± 0.5	43.6	2	2.23 ± 0.03	97 ± 2	
				76–102	64.6 ± 0.2	64.6	3	1.53 ± 0.13	99 ± 9	
Mean									98 ± 5	1.3
BRL	34°52.8′	116°13.4′	508	26–102	17.45 ± 0.02	17.45	17	2.76 ± 0.10	48 ± 2	1.4
BRN	34°53.6′	116°12.8′	469	30–101	22.41 ± 0.09	21.7	7	2.82 ± 0.12	61 ± 3	
Mean									55 ± 6	
FIN	35°29.3′	116°30.5′	1048	30–142	28.73 ± 0.05	28.20	25	3.33 ± 0.07	96 ± 2	2.0
AVA	35°35.5′	116°28.4′	579	53–101	31.02 ± 0.03	29.0	5	3.00 ± 0.14	87 ± •	2.7
FIS	35°12.3′	116°44.9′	951	31–91	21.60 ± 0.07	21.43	20	2.96 ± 0.03	63 ± 1	
				91–125	23.60 ± 0.10	23.44	11	2.99 ± 0.04	70 ± 1	
Mean									66 ± 4	1.2
GAR	35°27.8′	117°33.4′	1164	46–152	27.90 ± 0.03	28.6	24	3.09 ± 0.04	88 ± 1	2.1
FIC	35°21.1′	116°33.3′	756	30–102	33.7 ± 0.01	34.0	7	2.68 ± 0.05	91 ± 2	0.9
RMR	35°12.5′	117°50.3′	858	46–134	45.5 ± 0.05	45.5	8	3.03 ± 0.04	138 ± 2	4.5
FPK	35°15.5′	117°32.3′	936	61–102	23.71 ± 0.07	23.7	9	2.38 ± 0.06	56 ± 2	0.9
CBL	35°18.9′	117°20.2′	1146	46–76	26.05 ± 0.09	25.8	8	2.68 ± 0.04	69 ± 2	1.1
RGC	35°19.6′	117°37.5′	1070	21–160	29.12 ± 0.04	29.1	12	2.80 ± 0.08	82 ± 2	0.9
RGB	35°22.8′	117°21.8′	1015	90–153	29.74 ± 0.02	29.7	7	2.78 ± 0.06	83 ± 2	1.0
CQU	34°57.2′	118°17.1′	896	30–128	28.99 ± 0.01	29.0	8	3.19 ± 0.06	92 ± 2	2.2
CAJN‡	34°19.3′	117°28.7′	997	85–1788					69 ± 9	1.4
PSB	34°28.1′	117°51.2′	1076	61–152	27.22 ± 0.01	27.22	5	2.35 ± 0.12	64 ± 3	1.0
				152–245	29.80 ± 0.02	29.8	5	2.23 ± 0.14	66 ± 4	
PSBB§	34°28.1′	117°51.2′	1076	100–862					74 ± 2	1.0
PSC	34°33.2′	117°42.9′	933	46–213	20.51 ± 0.01	20.5	12	3.07 ± 0.14	63 ± 2	1.3
BBUT¶	34°33.0′	117°43.0′	928	122–644					69 ± 2	2.5
GMC	34°34.1′	117°06.4′	1030	61–152	23.41 ± 0.02	23.7	20	3.29 ± 0.10	78 ± 2	2.3
PSD	34°39.1′	117°50.8′	814	115–195	25.20 ± 0.05	25.2	13	2.61 ± 0.08	66 ± 2	2.1
HVI	34°43.9′	117°41.7′	928	65–107	22.10 ± 0.07	22.1	9	3.02 ± 0.06	67 ± 2	2.6
PSE	34°43.9′	117°41.7′	928	91–225	24.76 ± 0.03	24.8	8	2.77 ± 0.09	69 ± 2	2.6
STD	34°43.9′	117°04.4′	988	49–96	22.07 ± 0.02	22.1	11	2.86 ± 0.07	63 ± 3	2.9
HIVS	34°44.3′	117°46.4′	933	130–175	21.75 ± 0.05	21.8	3	2.91 ± 0.02	63 ± 1	
				175–274	24.28 ± 0.18	24.3	8	2.68 ± 0.04	65 ± 1	
				274–570	26.04 ± 0.01	26.0	25	2.50 ± 0.03	65 ± 1	
Mean									64 ± 1	
PSF	34°56.1′	117°45.7′	777	61–107	24.45 ± 0.05	24.5	11	2.81 ± 0.01	69 ± 3	2.4

See Figure 3 and A2. See also *Sass et al.* [1986, 1992] and *Lachenbruch and Sass* [1988].
*Γ_m, gradient calculated over stipulated depth range (plus or minus 95% confidence interval); Γ_c, corrected for steady state topography.
†N, number of specimens; ⟨K⟩, harmonic mean thermal conductivity (±95% confidence interval).
‡For details, see Table 4 of *Sass et al.* [1986].
§For details, see Table 2 of *Sass et al.* [1986].
¶For details, see Table 3 of *Sass et al.* [1986].

data from the southern Sierra Nevada by *Saltus and Lachenbruch* [1991], the western transverse range by *De Rito et al.* [1989], and previous studies of the San Andreas fault zone by *Lachenbruch and Sass* [1980], *Henyey* [1968], and *Henyey and Wasserburg* [1971] and of the Peninsular Range heat flow by *Roy et al.* [1972] and by *Lee* [1983] and *Combs* [1976]. The open circles in Figure 4 represent primarily the work of *Roy et al.* [1968b], *Warren et al.* [1969], *Sass et al.* [1971b], and *Shearer and Reiter* [1981]. Where gaps in the data remain, they are in terranes within which no suitable drill site could be found or in areas where access was impossible due either to the absence of roads or to restrictions imposed by government authorities.

The heat flow data of Figures 3 and 4 were contoured together with previously published data from adjoining western New Mexico (Figure 5). The contours outline several thermal features coincident with some of the major physiographic-tectonic units of the region. The range of heat flow is the same as that for other parts of the Western Cordillera. Moving from west to east, the Peninsular Range heat flow is essentially unchanged from the interpretations based on the work of *Henyey and Wasserburg* [1971], *Roy et al.* [1972] and *Lee* [1983]. Low heat flows in that province are generally attributed to Neogene compressional tectonics including Miocene subduction [*Roy et al.*, 1972; *Smith*, 1978].

As pointed out by *Lachenbruch et al.* [1978], heat flow within the Mojave Block is predominantly low (<80 mW m^{-2}) relative to the eastern Mojave which, for the purposes of this paper, includes the northwestern portion of the southern Basin and Range Province. The eastward transition to higher heat flow occurs across the southward extension of the Death Valley fault zone (the Soda Avawatz fault accord-

Table 4. Thermal Data for Crystalline Rocks of the Eastern Mojave Province, California, Arizona, and Nevada

Well Designation	Latitude N	Longitude W	Elevation, m	Depth Range, m	Gradient,* °C km^{-1}		Thermal Conductivity,† W m^{-1} K^{-1}		Heat Flow, mW m^{-2}	Heat Production, μW m^{-3}
					Γ_m	Γ_c	N	⟨K⟩		
CAT	34°21.1′	114°10.1′	145	91–114	24.5 ± 0.03	23.5	5	3.15 ± 0.20	74 ± 6	
				118–124	29.5 ± 0.2	28.7	3	2.15 ± 0.13	62 ± 4	
Mean									68 ± 6	1.4
SIG	34°28.4′	113°42.0′	585	23–53	34.72 ± 0.05	34.7	3	3.32 ± 0.10	115 ± 4	2.1
PPK	34°40.8′	114°40.8′	430	122–175	28.41 ± 0.07	28.4	5	3.36 ± 0.14	95 ± 4	3.7
DCH	34°43.9′	113°54.6′	1026	50–128	34.80 ± 0.07	34.8	10	2.87 ± 0.08	100 ± 3	5.1
KNG	35°07.7′	114°04.1′	952	91–152	29.38 ± 0.03	29.4	6	3.40 ± 0.10	100 ± 3	3.2
DAV	35°13.2′	114°33.3′	232	61–137	34.63 ± 0.04	34.6	6	3.48 ± 0.43	120 ± 3	2.6
VAL	35°22.1′	113°39.4′	1154	75–123	26.86 ± 0.02	25.2	5	3.14 ± 0.13	79 ± 4	1.0
PCK	35°24.3′	113°48.2′	1204	107–155	23.56 ± 0.01	24.1	7	3.47 ± 0.10	84 ± 3	2.3
RIVP	34°01.3′	114°35.6′	360	91–149	21.3 ± 0.2		6	3.71 ± 0.16	79 ± 4	
SAVA	34°15.9′	114°33.1′	416	61–122	28.14 ± 0.13	28.1	7	3.54 ± 0.13	100 ± 4	
				122–183	30.88 ± 0.26	30.9	6	3.50 ± 0.11	108 ± 4	
Mean									104 ± 4	2.4
TRTL	34°27.5′	114°50.1′	509	46–143	33.16 ± 0.03	33.2	8	2.90 ± 0.05	96 ± 2	
				143–186	37.97 ± 0.06	38.0	4	2.81 ± 0.05	107 ± 2	
Mean									102 ± 5	1.2
SNAG	34°31.1′	114°38.7′	466	46–128	29.44 ± 0.03	29.4	7	2.83 ± 0.08	83 ± 2	
				128–186	33.81 ± 0.02	33.8	6	2.87 ± 0.03	97 ± 1	
Mean									90 ± 7	1.2
RSS	34°43.8′	115°40.3′	948	73–108	41.94 ± 0.15	41.9	4	2.55 ± 0.10	107 ± 4	1.5
WSS	34°44.9′	115°39.2′	975	44–79	28.14 ± 0.04	28.14	9	3.08 ± 0.03	87 ± 1	1.4
GPS	34°48.5′	115°36.6′	1208	61–101	22.5 ± 0.08	22.0	10	2.96 ± 0.05	65 ± 1	2.0
GPN	34°48.7′	115°36.6′	1225	61–101	25.4 ± 0.03	24.5	4	3.29 ± 0.11	80 ± 1	2.1
Mean									72 ± 8	2.0
SHL	35°02.6′	115°02.4′	988	27–46	22.02 ± 0.18	22.02	3	2.93 ± 0.08	64 ± 2	1.1
TMT	35°08.0′	115°24.2′	1634	30–60	23.64 ± 0.09	23.64	18	3.14 ± 0.02	74 ± 1	1.1
SMS	35°08.0′	116°09.1′	372	35–102	27.49 ± 0.01	27.49	15	3.72 ± 0.03	102 ± 1	2.3
TPK	35°16.7′	115°33.9′	1611	35–98	24.99 ± 0.06	25.2	15	3.36 ± 0.04	85 ± 1	1.9
YGR	35°23.3′	115°53.3′	914	43–98	30.50 ± 0.25	30.5	16	3.37 ± 0.04	103 ± 1	1.2
HHL	35°24.9′	116°02.8′	561	27–104	31.05 ± 0.02	31.05	9	2.99 ± 0.06	93 ± 1	1.3
				104–138	33.11 ± 0.08	33.11	6	2.38 ± 0.06	79 ± 1	2.9
Mean									86 ± 7	3.0
MSS	35°34.2′	115°34.8′	1724	140–792	22.28 ± 0.01	25.72	31	3.22 ± 0.06	83 ± 1	1.8
OHMW	35°41.1′	116°53.7′	940	30–179	34.9 ± 0.2	34.9	14	2.48 ± 0.09	87 ± 3	2.2
ALXH	35°45.5′	116°03.9′	805	61–134	34.69 ± 0.05	34.69	6	2.88 ± 0.11	100 ± 3	
				137–174	30.44 ± 0.06	30.44	5	3.33 ± 0.03	101 ± 2	
Mean									100 ± 3	3.3
IBXP	35°47.4′	116°20.2′	625	30–192	30.17 ± 0.14	32.7	15	2.52 ± 0.06	82 ± 2	3.1
GRW	36°04.8′	116°29.8′	1000	30–102	30.71 ± 0.01	30.0	7	2.51 ± 0.06	75 ± 2	1.4
RGA	35°28.0′	117°37.6′	1045	85–161	30.26 ± 0.02	30.3	5	2.53 ± 0.08	77 ± 3	1.6
LMT	35°31.8′	117°39.2′	1012	34–106	37.95 ± 0.03	38.0	23	2.53 ± 0.03	96 ± 1	1.6
SPH	35°33.6′	117°35.1′	1006	30–101	15.97 ± 0.01	16.0	14	2.99 ± 0.04	48 ± 1	1.9
ELP	35°26.0′	117°53.5′	998	31–145	33.57 ± 0.04	31.0	5	2.68 ± 0.04	83 ± 2	0.7
GBS	36°16.0′	114°11.8′	1232	69–133	19.13 ± 0.10	19.1	8	3.48 ± 0.09	67 ± 1	2.8

See Figures 3, 4, A3, and A4.
*Γ_m, gradient calculated over stipulated depth range (±95% confidence interval); Γ_c, corrected for steady state topography.
†N, number of specimens, ⟨K⟩, harmonic mean thermal conductivity (±95% confidence interval).

ing to *Garfunkel* [1974] or the Granite Mountain fault of *Dokka* [1983]). This boundary also coincides with the easterly limit of active seismicity [*Smith*, 1978] and with a change from predominantly strike-slip to normal faulting. Data obtained since 1978 define a zone of high heat flow (>80 mW m^{-2}) in the vicinity of the Garlock fault, probably too large to be explained by conventional models of frictional heating. (For an assumed slip rate of 1 cm/yr and fault depth of 10 km, such models yield an anomaly of only 5–10 mW m^{-2} within 5–10 km of the fault [*Lachenbruch and Sass*, 1992, Figure 12].) Although such a frictional contribution to the Garlock fault anomaly cannot be ruled out, none is observed on the San Andreas fault where a similar calculation suggests it should be greater by a factor of 3 or 4. More likely the anomaly reflects thermal transients associated with late Tertiary igneous activity. The most conspicuous part of the Garlock fault anomaly is near the Randsburg volcanic area and a possibly related transtensional fault offset [*Aydin and Nur*, 1982; *Clark*, 1973].

The eastern Transverse Ranges are characterized by heat flow of 60 mW m^{-2} and lower. Like the Peninsular Ranges, they have been subjected to compressional deformation during the Neogene period. The crustal thickening associated with these processes would result in a transient lowering of heat flow. Also, elevated masses tend to be areas of ground water recharge. It is possible that subtle, but significant effects resulting from this process persist to depths much greater than those of our heat flow holes and result in

Table 5. Thermal Data for Crystalline Rocks of the Transverse Ranges, Peninsular Ranges, Tehachapi Mountains, and Salton Trough

Well Designation*	Latitude N	Longitude W	Elevation, m	Depth Range, m	Gradient,† °C km^{-1}		Thermal Conductivity,‡ W m^{-1} K^{-1}		Heat Flow, mW m^{-2}	Heat Production, μW m^{-3}
					Γ_m	Γ_c	N	⟨K⟩		
OGIL (S)	32°48.2′	114°46.7′	131	79–143	21.11 ± 0.19	21.1	6	2.91 ± 0.06	61 ± 2	3.0
PDR4 (S)	32°50.4′	114°48.3′	158	76–134	23.86 ± 0.30	23.9	5	2.72 ± 0.04	61 ± 3	
PDR2 (S)	32°50.5′	114°48.0′	162	100–116	23.62 ± 0.19	23.6	4	2.72 ± 0.06	65 ± 2	
KWD1 (P)	33°42.5′	116°42.9′	1492	100–307	19.94 ± 0.02	18.5	17	2.25 ± 0.04	42 ± 1	
PSA (Tr)	34°25.6′	117°51.8′	1301	71–229	34.87 ± 0.02	33.5	10	1.88 ± 0.05	63 ± 2	
GRM (Tr)	34°30.5′	118°16.8′	902	122–244	24.74 ± 0.01	22.9	6	2.49 ± 0.04	57 ± 2	0.9
TEH (Te)	35°08.3′	118°26.2′	1219	69–102	27.81 ± 0.07	27.8	8	3.12 ± 0.11	87 ± 4	1.8
HFM (Te)	35°21.6′	118°06.6′	1137	100–152	24.68 ± 0.02	23.2	8	2.39 ± 0.07	55 ± 2	1.1
CIN (Te)	35°18.3′	118°02.8′	975	116–171	25.90 ± 0.02	27.0	6	2.88 ± 0.05	78 ± 2	1.6

See Figures 3 and A5.

*Letters in parentheses after well designation denote physiographic tectonic province; S, Salton Trough; P, Peninsular Ranges; Tr, Transverse Ranges; and Te, Tehachapi Mountains.

†Γ_m, gradient calculated over stipulated depth range (±95% confidence interval); Γ_c, corrected for steady state topography.

‡N, number of specimens; ⟨K⟩, harmonic mean thermal conductivity (±95% confidence interval).

measured heat flows systematically lower than regional [*Bredehoeft and Papadopulos*, 1965; *Lachenbruch and Sass*, 1977]. However, under comparable conditions in the Sierra Nevada, such systematic hydrologic effects are ruled out by the remarkable linear relation between heat flow and surface radioactivity irrespective of elevation [*Roy et al.*, 1968a; *Lachenbruch*, 1968a, 1970; *Saltus and Lachenbruch*, 1991].

It is noteworthy that the 80 mW m^{-2} contour enclosing the Transverse Range low and its southeastward extension (Figure 5) also contains most of the outcrops of the Orocopia Schist, a subducted terrane. Mafic oceanic terranes are typically low in radiogenic heat production. The Orocopia Schist is mostly (70–99%) metagreywacke of continental origin with a subordinate to minor oceanic mafic component

Table 6. Thermal Data From the Sonoran Desert Region, Arizona Basin and Range

Well Designation	Latitude N	Longitude W	Elevation, m	Depth Range, m	Gradient,* °C km^{-1}		Thermal Conductivity,† W m^{-1} K^{-1}		Heat Flow, mW m^{-2}	Heat Production, μW m^{-3}
					Γ_m	Γ_c	N	⟨K⟩		
BMO1	32°02.8′	111°30.6′	884	85–157	40.08 ± 0.03	40.1	9	2.14 ± 0.05	86 ± 2	
AGU	32°05.6′	113°12.7′	332	30–151	92.94 ± 0.06	92.9	10	3.59 ± 0.11	334 ± 10	2.5
QJT	32°07.6′	112°07.9′	811	38–146	26.65 ± 0.06	26.7	10	2.90 ± 0.11	77 ± 3	1.4
BMO2	32°09.3′	112°39.4′	677	46–91	29.35 ± 0.03	29.4	9	2.83 ± 0.08	83 ± 2	
CAB	32°19.9′	112°55.9′	554	110–154	30.92 ± 0.21	30.9	11	3.04 ± 0.10	94 ± 3	1.8
MHK	32°43.9′	113°45.0′	168	91–160	24.0 ± 0.05	23.5	5	2.97 ± 0.10	70 ± 2	1.3
AZT	32°46.5′	113°27.5′	178	55–153	26.85 ± 0.05	26.7	10	2.37 ± 0.05	63 ± 1	0.6
TTP	32°50.0′	112°09.9′	581	40–150	22.40 ± 0.10	22.4	10	3.41 ± 0.12	76 ± 6	3.3
CGA	32°53.8′	111°52.8′	403	381–491	21.2 ± 0.3					
CGB	32°53.7′	111°52.8′	403	332–477	23.3 ± 0.1	22.4	6	3.60 ± 0.16	81 ± 4	
CGC	32°53.7′	111°52.8′	403	427–553	22.8 ± 0.2					
ASC	32°57.9′	111°48.7′	446	485–545	19.49 ± 0.03	20.1	14	3.47 ± 0.14	70 ± 5	
ASD				483–500	20.7 ± 0.1					
ALP	32°59.3′	111°06.8′	820	61–107	23.12 ± 0.2	23.1	8	3.32 ± 0.05	76 ± 2	1.8
MCP	32°59.6′	112°31.5′	375	100–177	34.60 ± 0.05	34.6	6	3.77 ± 0.10	130 ± 3	1.6
GMT	33°09.8′	111°03.0′	787	125–155	33.05 ± 0.05	32.0	6	2.66 ± 0.11	85 ± 4	1.1
YMB	33°14.2′	113°11.4′	402	73–139	25.90 ± 0.04	25.9	6	2.88 ± 0.09	75 ± 2	0.8
BUC	33°18.7′	112°36.4′	262	61–122	7.89 ± 0.02	7.9	6	3.95 ± 0.08	31 ± 1	1.8
TRG	33°25.5′	114°28.2′	262	91–160	34.66 ± 0.02	34.7	9	2.63 ± 0.16	91 ± 6	0.8
GRN	33°31.5′	111°39.5′	443	30–152	23.22 ± 0.04	23.2	11	3.32 ± 0.05	77 ± 2	1.5
QZTW	33°39.4′	114°19.7′	390	53–107	27.7 ± 0.10	27.7	7	3.44 ± 0.06	95 ± 2	
AGLA	33°44.5′	113°07.2′	762	125–204	22.6 ± 0.2	22.6	11	2.68 ± 0.04	61 ± 1	
LHR	33°44.8′	113°39.0′	610	107–152	25.55 ± 0.05	25.6	4	3.15 ± 0.03	80 ± 2	2.2
CFR	33°50.1′	111°50.2′	989	88–153	21.82 ± 0.02	21.8	6	3.50 ± 0.08	76 ± 2	3.4
VUL	33°52.2′	112°49.8′	756	79–151	20.40 ± 0.04	20.1	5	2.88 ± 0.09	58 ± 2	1.6
BOU	33°56.0′	113°53.7′	393	122–152	27.03 ± 0.04	27.0	9	2.81 ± 0.13	76 ± 4	1.4
CON	34°00.7′	112°38.7′	901	44–111	18.1 ± 0.13	18.1	5	2.65 ± 0.12	48 ± 3	2.1
MRT	34°06.4′	112°59.3′	847	107–166	28.41 ± 0.05	28.0	4	2.94 ± 0.17	82 ± 5	2.6

See Figures 4 and A6.

*Γ_m, gradient calculated over stipulated depth range (±95% confidence interval); Γ_c, corrected for steady state topography.

†N, number of specimens; ⟨K⟩, harmonic mean thermal conductivity (±95% confidence interval).

Table 7. Thermal Data From the Arizona Transition Zone

Well Designation	Latitude N	Longitude W	Elevation, m	Depth Range, m	Gradient,* °C km^{-1}		Thermal Conductivity,† W m^{-1} K^{-1}		Heat Flow, mW m^{-2}	Heat Production, μW m^{-3}
					Γ_m	Γ_c	N	⟨K⟩		
BMS	33°51.0′	111°28.4′	1115	67–147	25.53 ± 0.01	25.3	6	3.37 ± 0.04	86.2 ± 2	2.1
DCR	34°14.4′	112°52.1′	1024	43–109	23.55 ± 0.04	23.6	5	3.36 ± 0.09	79 ± 2	2.6
PAY	34°15.4′	111°16.7′	1462	96–152	22.05 ± 0.04	22.0	5	3.28 ± 0.16	72 ± 4	1.7
CRD	34°16.9′	112°06.8′	1103	30–110	17.30 ± 0.04	16.8	7	3.70 ± 0.08	62 ± 2	0.5
WLH	34°25.0′	112°34.8′	1512	46–158	31.91 ± 0.04	31.9	8	2.88 ± 0.08	92 ± 3	0.8
AST	34°27.7′	113°15.3′	853	97–152	27.10 ± 0.02	26.9	5	3.10 ± 0.11	83 ± 3	3.8
PRS	34°29.8′	112°27.9′	1759	88–127	33.06 ± 0.10	31.0	4	2.73 ± 0.03	85 ± 2	0.6
MUL	34°30.3′	112°54.5′	1109	30–146	25.34 ± 0.02	25.3	9	3.19 ± 0.11	81 ± 3	4.4
CHR	34°32.6′	112°04.2′	1463	61–152	20.00 ± 0.01	20.0	9	3.08 ± 0.04	62 ± 1	0.4
BGD1	34°34.9′	113°13.1′	1042	183–503	29.51 ± 0.01	29.5	19	2.79 ± 0.02	82 ± 1	2.5
CPWD	34°47.4′	112°54.7′	1786	67–154	35.81 ± 0.09	35.8	8	3.31 ± 0.03	119 ± 1	4.0
CHNO	34°47.5′	112°17.1′	1576	46–159	21.50 ± 0.07	21.5	10	2.78 ± 0.08	60 ± 2	0.7
WNT	34°54.5′	112°50.5′	1600	46–152	30.87 ± 0.04	30.9	9	3.66 ± 0.05	113 ± 2	2.8
CRMT	35°11.5′	113°22.9′	1525	41–93	30.12 ± 0.05	30.1	5	3.41 ± 0.05	103 ± 2	4.1
CHN	35°23.9′	112°53.0′	1463	85–150	36.24 ± 0.02	36.2	9	3.16 ± 0.03	115 ± 1	3.5

See Figures 4 and A7.
*Γ_m, gradient calculated over stipulated depth range (±95% confidence interval); Γ_c, corrected for steady state topography.
†N, number of specimens; ⟨K⟩, harmonic mean thermal conductivity (±95% confidence interval).

Table 8. Thermal Data From the Mexican Highlands, Arizona Basin and Range

Well Designation	Latitude N	Longitude W	Elevation, m	Depth Range, m	Gradient*, °C km^{-1}		Thermal conductivity,† W m^{-1} K^{-1}		Heat Flow, mW m^{-2}	Heat Production, μW m^{-3}
					Γ^m	Γ_c	N	⟨K⟩		
NOG	31°22.7′	110°45.5′	1433	110–152	35.40 ± 0.02	34.5	11	2.63 ± 0.04	91 ± 2	4.2
TBS	31°41.2′	110°06.6′	1338	40–152	25.77 ± 0.09	25.8	11	3.04 ± 0.07	78 ± 2	1.6
RIN	32°04.4′	110°39.5′	1077	70–150	21.64 ± 0.02	21.6	11	3.16 ± 0.05	68 ± 1	1.6
DOS	32°10.7′	109°35.3′	1628	75–140	16.21 ± 0.08	15.6	11	3.29 ± 0.09	51 ± 2	3.3
CAS	32°12.2′	110°14.0′	1324	65–134	21.6 ± 0.1	21.6	10	3.24 ± 0.06	70 ± 1	1.8
TOR	32°30.8′	110°59.8′	1060	30–146	20.34 ± 0.02	20.3	10	2.32 ± 0.11	47 ± 2	2.1
PNA	32°33.4′	109°44.8′	1347	35–152	36.50 ± 0.10	34.7	10	3.08 ± 0.02	107 ± 2	2.8
BMT	32°47.0′	110°55.4′	1327	35–78	17.14 ± 0.14	17.1	5	3.72 ± 0.08	64 ± 2	2.8
TLR	32°50.2′	110°07.3′	1334	94–141	24.3 ± 0.1	24.3	10	3.47 ± 0.12	84 ± 3	1.9
PNT	33°21.3′	110°57.8′	1422	61–152	19.25 ± 0.09	19.2	8	2.86 ± 0.03	55 ± 1	0.9

See Figures 4 and A8.
*Γ_m, gradient calculated over stipulated depth range (±95% confidence interval); Γ_c, corrected for steady state topography.
†N, number of specimens; ⟨K⟩, harmonic mean thermal conductivity (±95% confidence interval).

Table 9. Summary of Heat Flow Data From NURE Wells, Arizona

Hole	Latitude N	Longitude W	Elevation, m	Depth Range, m	Heat Flow, mW m^{-2}	Heat Production,* μW m^{-3}
PQ-3	34°00.3′	113°13.1′	662	122–1317	79	1.42
PQ-1	34°07.8′	112°51.5′	891	122–905	70	2.44
PQ-4	34°09.4′	113°10.6′	759	244–1646	68	
PQ-8	34°17.0′	113°56.6′	267	274–625	70	4.26
PQ-9	34°38.5′	113°58.6′	683	244–1574	92	7.69

See *Sass et al.*, [1981b].
*Single determinations on basement core when basement penetrated.

Table 10. Summary of Heat Flow Estimates From the Colorado Plateau of NE Arizona

Hole	Latitude N	Longitude W	Elevation, m	Depth Range, m	Heat Flow, mW m^{-2}
TGE-3	34°18.0′	109°23.4′	2033	343–400	63
TGE-1	34°19.3′	109°16.6′	1989	244–420	76
TGE-2	34°20.6′	109°14.3′	2039	171–225	79
CVL	34°32.4′	110°55.6′	2143	46–167	39
PWF3	34°33.9′	109°18.3′	1787	75–200	86
PWF1	34°34.1′	109°17.2′	1777	35–85	149
PWF2	34°34.2′	109°21.5′	1723	15–85	116
WFA	34°52.2′	111°24.7′	2329	91–219	6
FWT	35°00.6′	111°17.4′	1953	122–533	28
WOM	35°01.0′	111°17.3′	1949	457–576	25
WOT	35°03.1′	111°35.9′	2187	128–250	4
LM01	35°07.3′	111°35.7′	2085	174–331	9
ALTO	35°12.2′	111°27.7′	1963	98–488	41
SMT7	35°20.5′	111°43.7′	2588	61–104	51
SSCR	35°22.1′	111°34.6′	2124	274–588	24
WIDE	35°23.6′	109°31.3′	1861	210–314	110
BMPS	35°31.6′	112°09.8′	1879	61–415	32
CRNS	35°34.2′	111°28.7′	1640	152–506	20
RBDX	35°39.2′	112°08.4′	1826	201–402	53
CORN	35°39.7′	109°36.7′	1924	100–335	94
GRAY	35°45.8′	111°29.7′	1501	250–320	14
HARD	36°02.6′	110°31.6′	1823	185–520	62
PIN1	36°05.5′	110°12.4′	1930	60–466	50
INSC	36°36.2′	110°48.8′	1963	91–183	65
BMSA	36°38.8′	110°10.1′	1723	50–400	61

See *Sass et al.* [1982].

[*Haxel et al.*, 1987]. Geochemical studies of the Orocopia Schist [e.g., *Haxel et al.*, 1987] indicate that they have average upper crustal abundances of the heat-producing elements and are thus not, in themselves, the origin of this relative heat flow low. Structural studies of their emplacement, however, suggest that they were tectonically buried on a subducting plate associated with a collided microcontinental fragment or rapid low-angle subduction [*Dillon et al.*, 1990]: The crust beneath the Orocopia Schist may therefore be atypical of adjacent crust. If this crust contains an atypically high mafic component, as suggested by its subduction-related origin, the relative heat-flow low may be associated with low total crustal heat production as mafic rocks are generally low in heat production [*Rybach*, 1988]. Additional studies are clearly required to investigate the origin of this anomaly.

The Salton Trough (contained within the 100 mW m^{-2} contour of Figure 5) is an evolving extensional sedimentary basin. The high heat flow, which averages ~150 mW m^{-2} and exceeds 1 W m^{-2} in some areas [*Sass et al.*, 1984a, 1988b; *Newmark et al.*, 1988] can be explained in terms of rapid extension, subsidence, and sedimentation, with basaltic underplating of a thin crust/lithosphere (~25 km) and the accompanying magmatic and hydrothermal processes [*Lachenbruch et al.*, 1985].

With the exception of an elongate zone of lower-than-average heat flow corresponding to the major trend of the metamorphic core complexes [*Coney*, 1980] discussed at length below, the heat-flow distribution in the remaining Basin and Range subprovinces and the Arizona Transition Zone (Figure 5) is very similar to other parts of the Basin and Range. The heat flow distribution for the southern Colorado Plateau is unexpected in view of the Pliocene and Holocene igneous activity in the region.

Heat Flow and Late Tertiary Igneous Activity

Blackwell [1978] postulated that in areas subjected to volcanism younger than 17 Ma, the surface heat flow has a component contributed by thermal transients that accompanied the volcanic activity. To test this hypothesis, we superimpose the distribution of igneous rocks younger than 17 Ma [*Stewart and Carlson*, 1978] on our heat flow contour map (Figure 6). Despite the near absence of surface manifestations, the Salton Trough (as we have mentioned) is an evolving sedimentary basin having high rates of extension and magmatic underplating and intrusion [*Lachenbruch et al.*, 1985]. Regions of high (>80 mW m^{-2}) heat flow in the Sonoran Desert, Eastern Mojave, and Transition Zone also are sometimes associated with middle Miocene and younger volcanic activity, as are the high heat-flow zones associated with the Garlock and Death Valley fault zones. On the Colorado Plateau proper, there is a high heat flow zone associated with young volcanism in the Southeast (Figure 6). In contrast, the San Francisco Volcanic Field near Flagstaff is nearly all within the 60 mW m^{-2} contour even though there has been active volcanism there within the past 1000 years [*Smiley*, 1958] and evidence from teleseismic *P* wave residuals indicates the presence of a magma chamber beneath the field [*Stauber*, 1982]. Thus, although some regions of mid-Miocene and younger volcanic activity are associated with high heat flow, others are not, and some regions whose youngest magmatic activity is middle Tertiary or older have high heat flow. In addition, there are areas where deep-seated hydrologic processes are most likely responsible for the observed heat flow.

The Great Basin (or northern Basin and Range) is nearly a kilometer higher in average elevation than the Mojave-Sonoran region (the southern Basin and Range) and has been

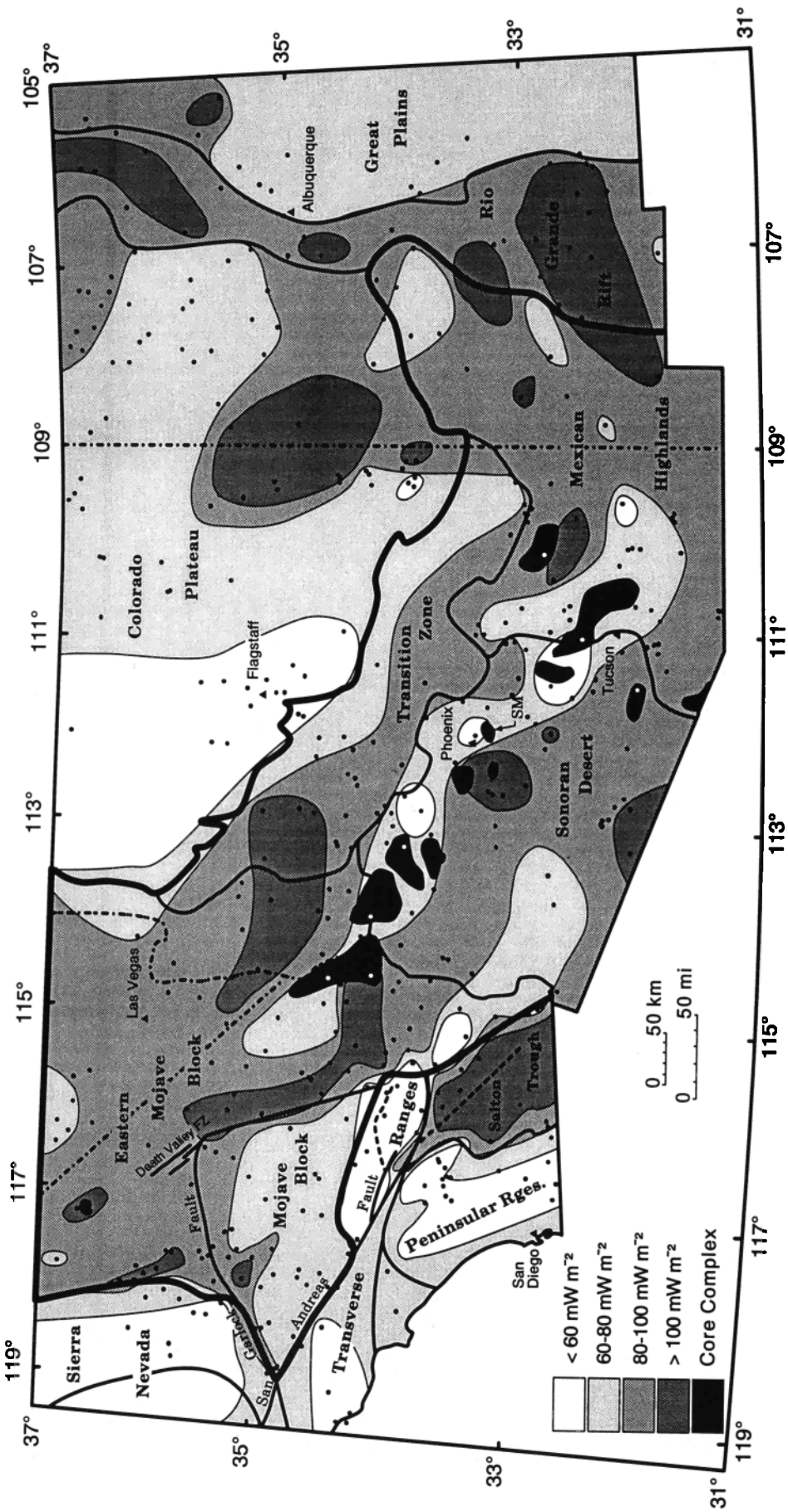

Figure 5. Heat flow contour map of southern California, Nevada, Arizona, and western New Mexico. Contour interval 20 mW m^{-2}. Metamorphic core complexes from Figure 1 of *Coney* [1980] with minor modifications in southernmost Arizona (G. B. Haxel, personal communication, 1990).

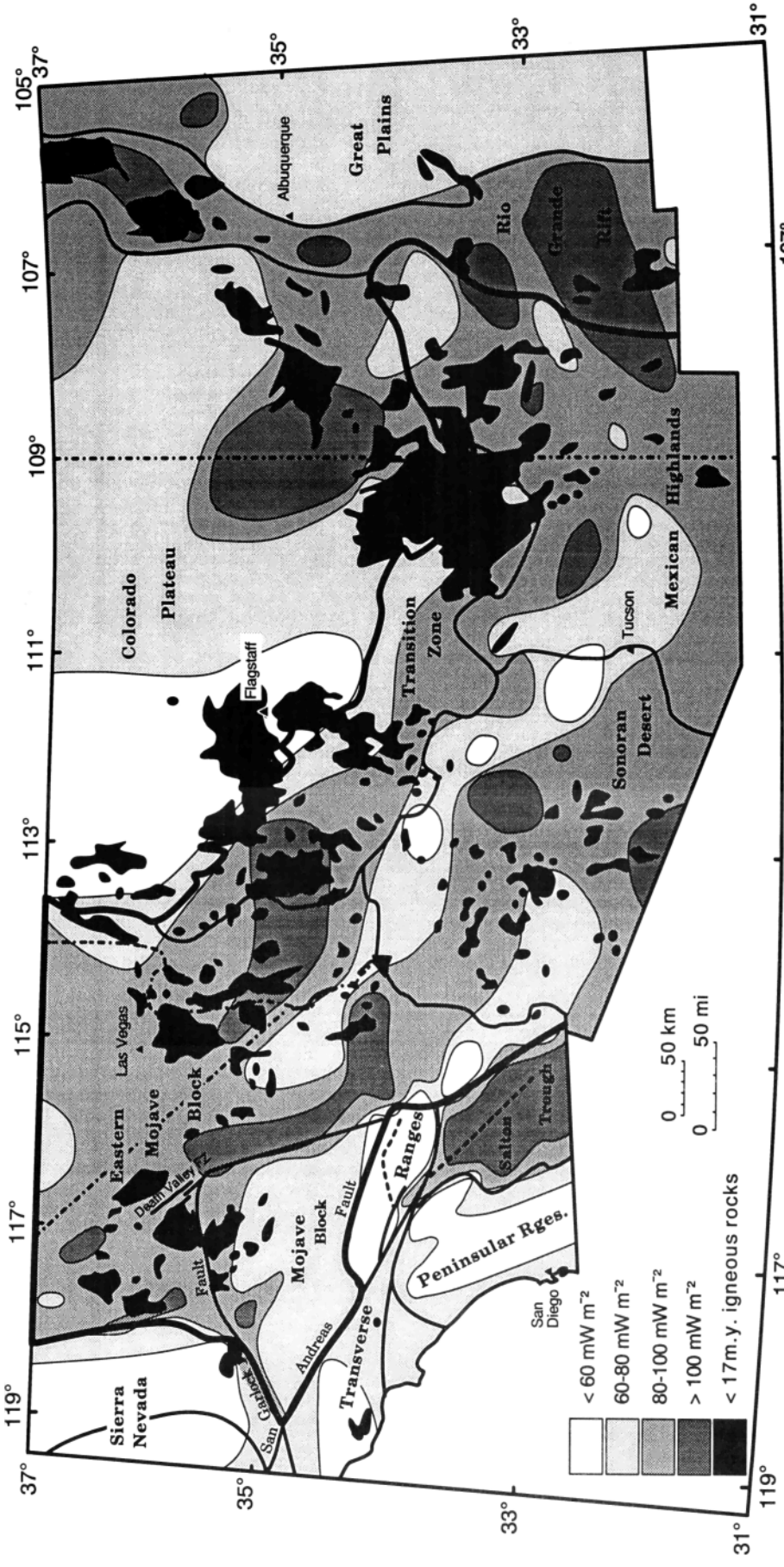

Figure 6. Heat flow contours in relation to igneous activity younger than 17 Ma [*Stewart and Carlson*, 1978].

Table 11. Mean Heat Flows and ±95% Confidence Limits From Crystalline Rocks Within the Basin and Range Province

Province	Number of Sites	Mean Heat Flow, mW m^{-2}					Mean Elevation, m
		Total	<17 m.y.		>17 m.y.		
			n	q	n	q	
Basin and Range	214	84 ± 3	90	87 ± 4	124	83 ± 5	1158 ± 75
Northern Basin and Range	57	92 ± 9	25	86 ± 10	32	97 ± 15	1793 ± 77
Southern Basin and Range	157	82 ± 3	65	87 ± 4	92	78 ± 4	918 ± 66
Mojave Block	30	76 ± 6	9	77 ± 7	21	76 ± 7	939 ± 69
Eastern Mojave	58	87 ± 5	30	90 ± 5	28	84 ± 9	770 ± 114
AZ Transition Zone	19	86 ± 10	14	86 ± 10	5	81	1336 ± 145
Sonoran Desert	25	79 ± 7	11	87 ± 11	14	73 ± 9	557 ± 103
Mexican Highlands	25	76 ± 6	1	55	24	77 ± 6	1210 ± 124

Excluding Salton Trough and Rio Grande Rift.

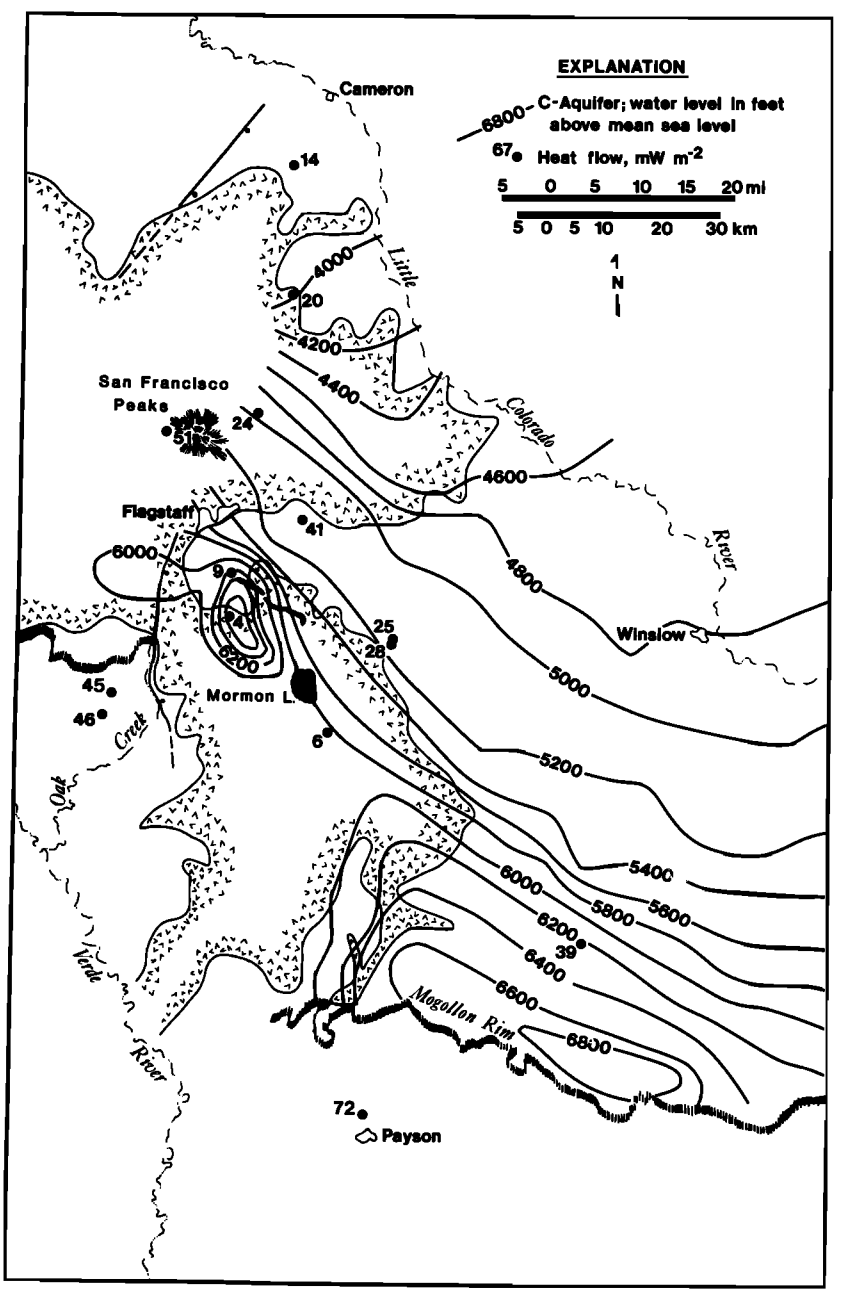

Figure 7. North central segment of Figure 4 showing the outline of the San Francisco Volcanic Field (pattern), the southern physiographic boundary of the Colorado Plateau (Mogollon Rim), water level contours on the Coconino aquifer [*Appel and Bills*, 1980, 1981], and heat flow values.

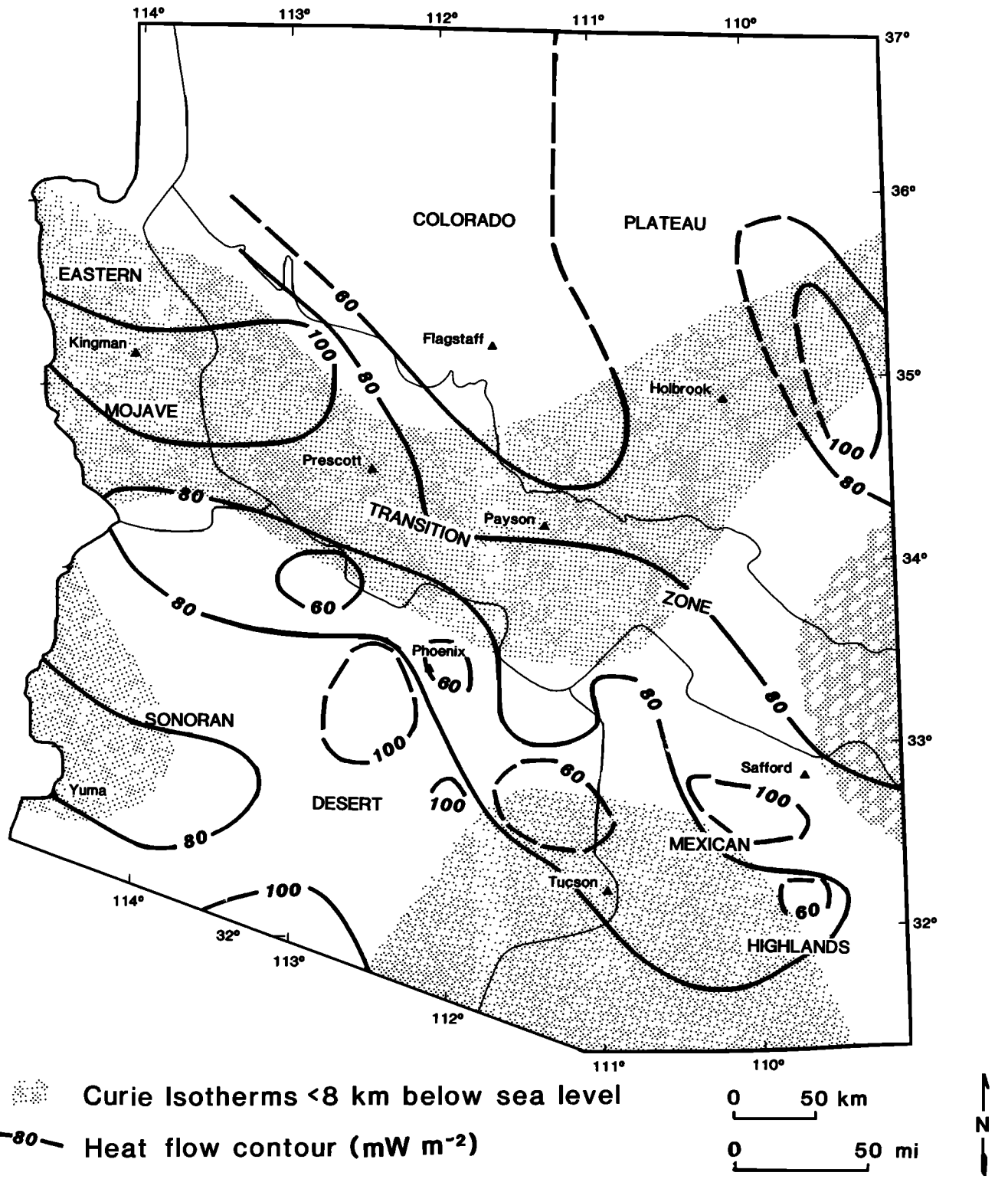

Figure 8. Contour map of Arizona heat flow showing the zones of relatively shallow (<8 km below sea level) depth-to-Curie isotherm as interpreted by *Hong et al.* [1981].

extending throughout much of the past 30 m.y. including the present [*Coney and Harms*, 1984; *Mayer*, 1986; *Gans et al.*, 1989], whereas the Mojave-Sonoran region has been relatively stable for the past 10 to 15 m.y. [*Dokka*, 1989; *Spencer and Reynolds*, 1991]. If we consider the two regions separately, we see little evidence for a heat flow anomaly associated with <17 m.y. igneous rocks. In fact, for the northern Basin and Range, the mean heat flow associated with >17 m.y. rocks is higher (although not significantly so) than for the general population. Overall, the difference in heat flow between subprovinces of igneous rocks greater than and less than 17 m.y. old is not significant at the level of

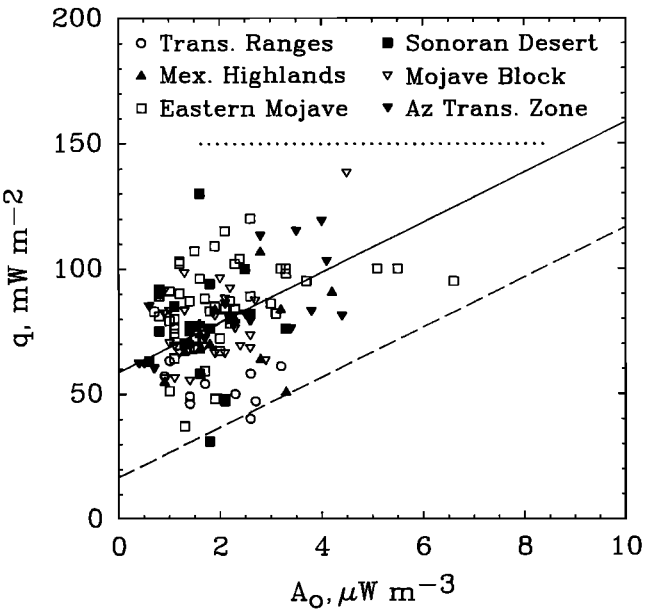

Figure 9. Heat flow q versus radiogenic heat production A_0 for the Basin and Range Province of California, southernmost Nevada (Figure 3), and Arizona (Figure 4); solid line, Basin and Range reference line; dashed line, Sierra Nevada.

95% confidence. The same is true (Table 11) of the difference between all points in the northern Basin and Range (92 ± 9, ±95% confidence level, n = 57) and the southern Basin and Range (82 ± 3, n = 157).

Effects of Hydrologic Processes

Because the majority of wells used in this study were dedicated drill holes with casing grouted in, there is little evidence for thermal disturbances by moving water in the temperature profiles of the appendix.

Extremely low heat flow is found near Flagstaff on the southern margin of the Colorado Plateau (inner rectangle, Figure 4) within and adjacent to the San Francisco Volcanic Field which has been active as recently as Holocene time [*Reynolds et al.*, 1986]. With the widespread extensional and igneous activity associated with the Colorado Plateau margin, we should expect to observe high heat flow akin to that observed to the east (Figures 4, 5, and 6). Elevated heat flow was indicated in this region by estimates of heat flow from the silica content of groundwater by *Swanberg and Morgan* [1980]. A plausible explanation for the low measured heat flow can be found in hydrologic studies [*Levings and Mann*, 1980; *Appel and Bills*, 1980, 1981]. The Coconino Sandstone is the major regional aquifer. Water level contours dip systematically to the northeast (Figure 7) with very steep lateral gradients in areas of single-digit heat flow. There is abundant spring discharge in both the Colorado and Little Colorado Rivers [*Cooley*, 1976; *Cooley et al.*, 1969; *Johnson and Sanderson*, 1968; *Huntoon*, 1981]. Thus it is reasonable to suppose that large amounts of heat are being carried laterally and discharged in large volume springs whose temperatures are only a few degrees above ambient.

Heat Flow and Curie Isotherms in Arizona

The depth of the Curie isotherm (~580°C) is a function of the local geotherm and thus, should be related to the heat

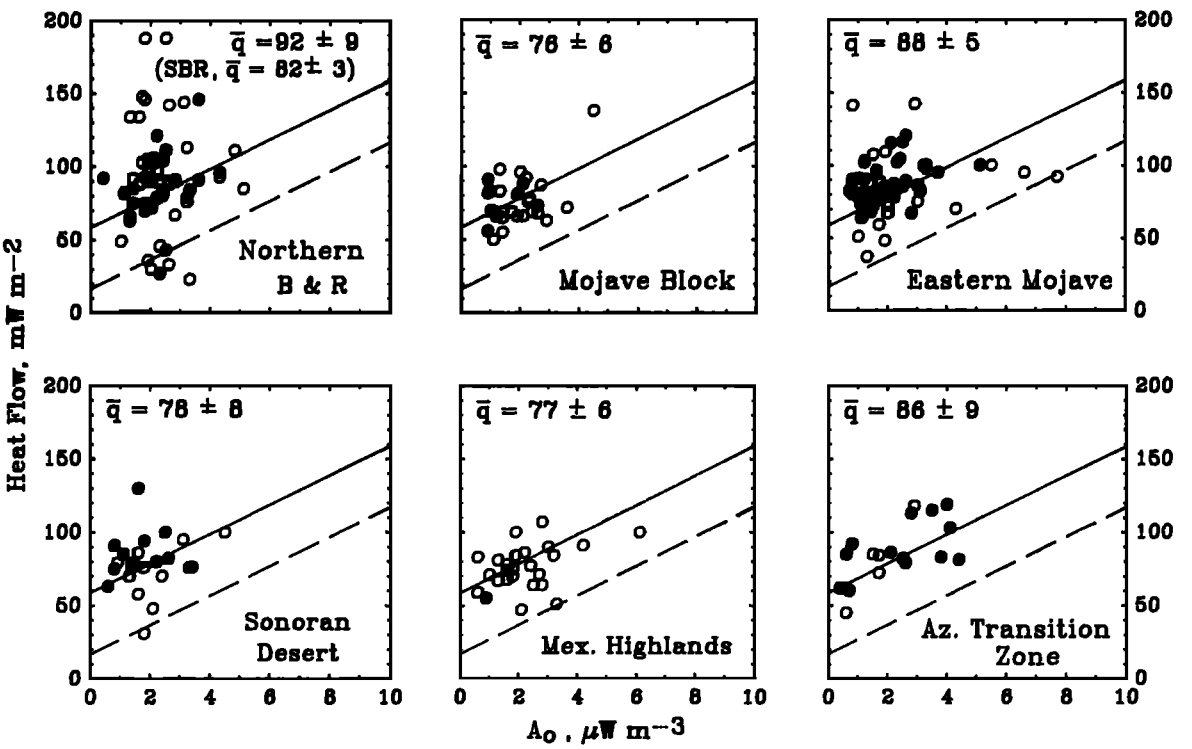

Figure 10. Heat flow–heat production plots for individual tectonic units, together with Basin and Range (solid) and Sierra Nevada (dashed) reference lines. Solid dots are for sites located within 10 km of a 17 Ma or younger igneous body.

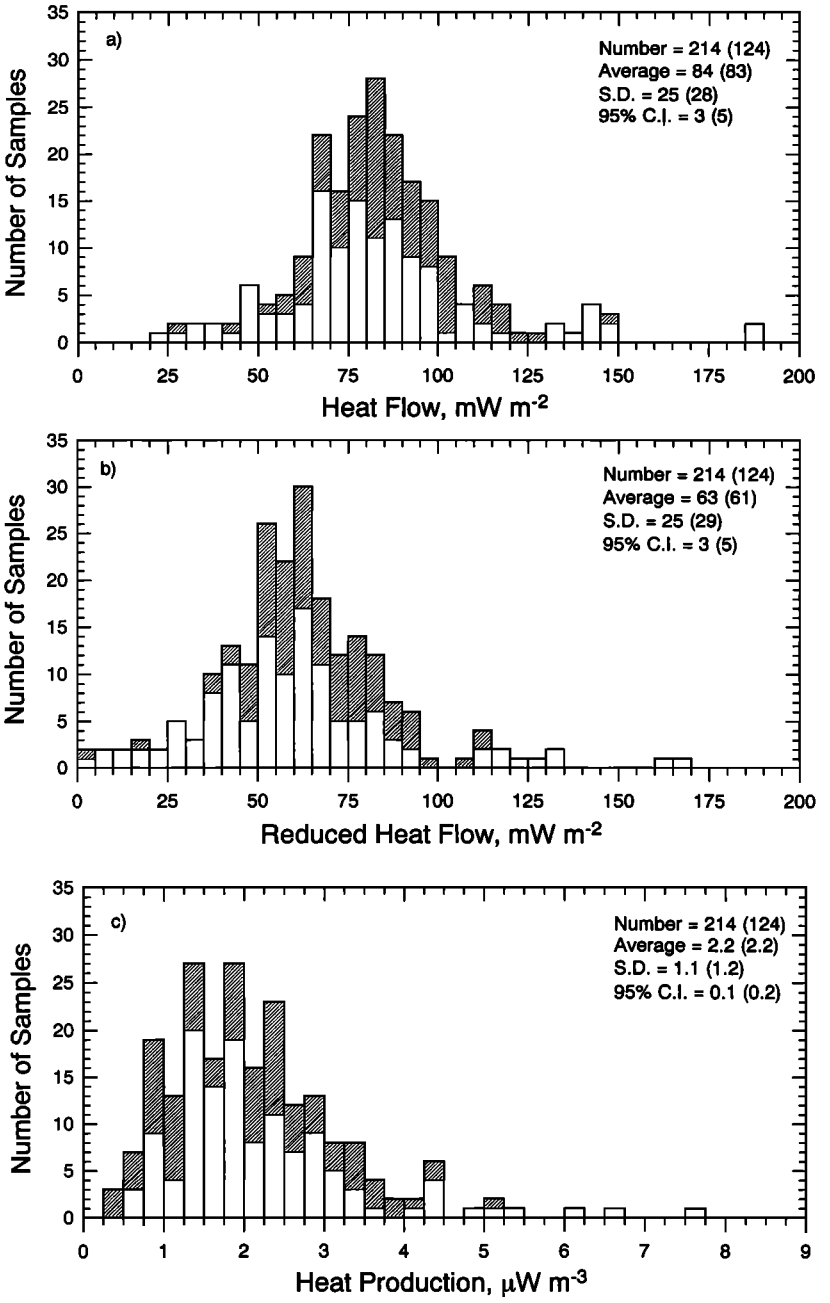

Figure 11. Histograms of (a) heat flow, (b) reduced heat flow, and (c) radioactive heat production for stations at which both q and A_0 were measured in the Basin and Range Province (excluding the Salton Trough and the Rio Grande Rift). Shaded portions of histograms indicate data obtained from sites within 10 km of igneous bodies younger than 17 Ma. Statistics in parentheses exclude the latter data.

flow. We know of no estimates of this quantity for southern California, but two estimates have been made for Arizona. *Byerly and Stolt* [1977] performed a spectral analysis of total intensity aeromagnetic data, from which they inferred that there is a zone of relatively shallow Curie isotherms (<10 km) corresponding to the Arizona Transition Zone which is characterized by high heat flow, >80 mW m^{-2} (Figure 8). *Hong et al.* [1981] using inversion techniques, obtained results compatible with those of Byerly and Stolt in the Transition Zone and found evidence for additional highs in southern Arizona. These latter anomalies seem to correspond more with zones of low than of high heat flow. They are thus likely to be the result of something other than high crustal temperatures.

Heat Flow and Heat Production

For certain tectonic provinces [*Birch et al.*, 1968; *Roy et al.*, 1968a; *Lachenbruch*, 1968a, 1970], there is a linear relation ($q = q^* + DA_0$) between heat flow (q) and surface heat production (A_0) from which it is possible to derive refined estimates of crustal geotherms. The intercept heat flow q^* is commonly interpreted as a measure of the heat flow from below a layer of laterally varying heat production and the slope D as a "characteristic depth" from which the

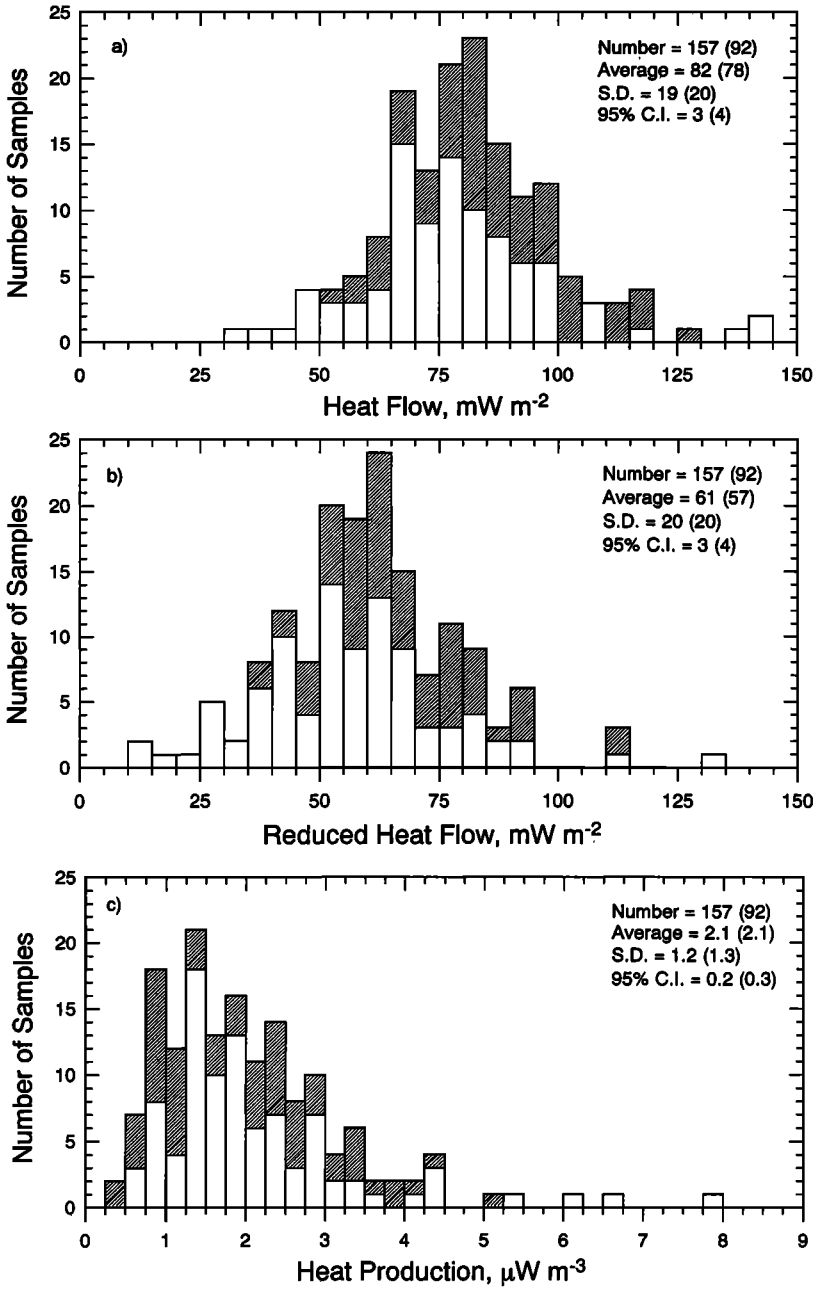

Figure 12. Histograms of (a) heat flow, (b) reduced heat flow, and (c) radioactive heat production for stations at which both q and A_0 were measured in the southern Basin and Range Province. Shaded portions of histograms indicate data obtained from sites within 10 km of igneous bodies younger than 17 Ma. Statistics in parentheses exclude the latter data.

thickness of the upper layer can be determined. Somewhat fortuitously, with their early data *Roy et al.* [1968a] were able to define a linear heat flow–heat production ($q - A_0$) relation for the plutonic crystalline rocks of the Basin and Range Province. The intercept on the heat flow axis was 59 mW m^{-2} and the slope was 9.4 km.

As more data accumulated, the original $q - A_0$ correlation for the Basin and Range Province deteriorated (compare Figure 5 of *Roy et al.* [1968a] and Figure 17 of *Lachenbruch and Sass* [1977]), and a statistically valid correlation was no longer possible. This is in contrast to the adjacent Sierra Nevada province for which values of reduced heat flow (defined as $q - DA_0$) are still grouped tightly about the mean [*Saltus and Lachenbruch*, 1991]. The $q - A_0$ relation from the southern Basin and Range Province and neighboring Transverse Ranges (Figures 3 and 4) is shown in Figure 9. No correlation is evident for the region as a whole, or for any physiographic region within it (Figure 10). The Transverse Ranges points lie below the Basin and Range reference line (Figure 9) reflecting the lower heat flow in this region.

Lachenbruch and Sass [1977] noted that $q - A_0$ pairs from the Battle Mountain High (BMH, Figure 1) plotted consistently above *Roy et al.*'s [1968a] line and that data from the Eureka Low (EL, Figure 1) plotted below that line.

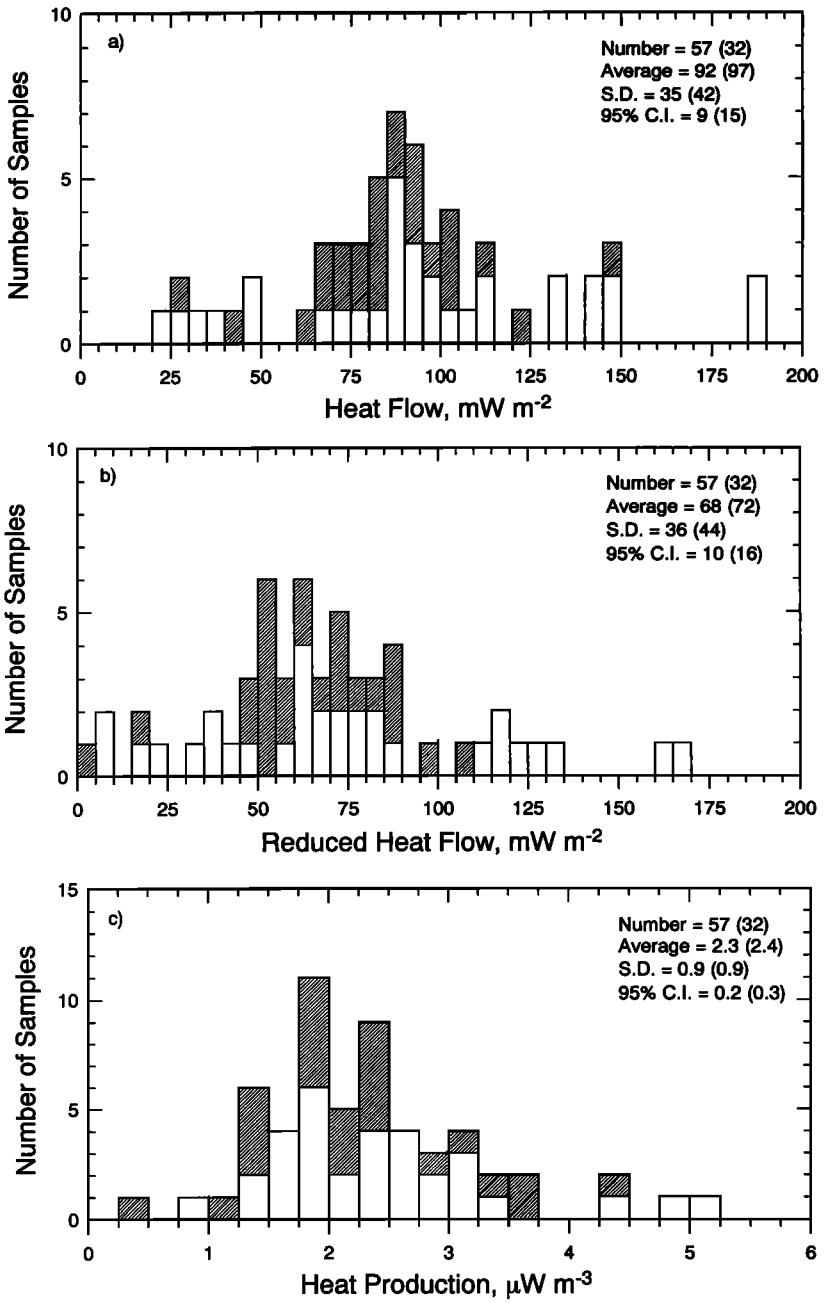

Figure 13. Histograms of (a) heat flow, (b) reduced heat flow, and (c) radioactive heat production for stations at which both q and A_0 were measured in the northern Basin and Range. Shaded portions of the histograms indicate data obtained from sites within 10 km of igneous bodies younger than 17 Ma. Statistics in parentheses exclude the latter data.

Their interpretation of these results was that convection, both magmatic and hydrologic (hydrothermal and otherwise), were overwhelming the conductive thermal regime. *Blackwell* [1978] acknowledged the scatter in the Basin and Range data and postulated that if all data from regions subjected to volcanic activity within the last 17 m.y. in a larger heat flow province he defined as a "Cordilleran Thermal Anomaly Zone" (CTAZ) were excluded, the remaining $q - A_0$ data plotted in a field that was consistent with the original Basin and Range line. Many of the plutons from which $q - A_0$ pairs were obtained had quite small (~1 to 10 km^2) surface exposures and subsurface geometries that were uncertain. At least some of the scatter could thus be attributed to lateral heat flow causing departures from quasi-one-dimensional models of the radioactive layer. An additional complication within the present study area arises from the fact that, owing to a combination of Mesozoic thrusting, Cenozoic extension, and in the Transverse Ranges–Western Mojave region, Neogene strike-slip and compressional tectonism, there are very few autochthonous intrusive bodies. Thus, if we assume that the vertical distribution of radioelements arises from differentiation of a substantial fraction of the crust, an assumption consistent with the simple crustal models [*Lachenbruch*, 1970], some additional departures

Table 12. Heat Flow and Heat Production in the Southern Basin and Range

	Heat Flow, mW m^{-2}				Heat Production, μW m^{-3}			
	Value	S.D.	95% C.I.	Number of Sites	Value	S.D.	95% C.I.	Number of Samples
A, Southern Basin Range (SBR)	83	20	2.6	234	2.1	1.2	0.2	157
B, SBR (excluding MCCL)	86	20	2.8	193	2.1	1.3	0.2	128
C, MCCL (heat-flow sites)	67	11	3.5	41	1.9	0.8	0.3	29
D, NURE MCC samples					1.3	1.0	0.3	108

A, all heat flow sites within the SBR province. B, SBR heat flow sites outside the metamorphic core complex low (MCCL). C, heat flow sites within the MCCL. D, Samples collected as part of the National Uranium Resource Evaluation (NURE) [see *Coney and Reynolds*, 1980]).

from the hypothesized linear $q - A_0$ relation should be expected.

It is instructive to examine the $q - A_0$ relationship within the context of Tertiary tectonic style and late Cenozoic igneous activity. In Figure 10, we show the relation for individual tectonic provinces and differentiate between those sites that have been subject to the effects of igneous activity younger than 17 m.y. and those that have not. Results from the northern Basin and Range, a province of higher elevation and younger extension are shown for comparison. It should be noted that our approach is somewhat different from that of *Blackwell* [1978]. In his Figure 8-3, Blackwell divided the CTAZ into large generalized zones belonging to particular age intervals for volcanic rocks. To distinguish igneous rocks younger or older than 17 Ma, we used the map of Figure 6. If a given point were within 10 km of one of the mapped bodies, we put it in the <17 m.y. population; otherwise, we left it in the >17 m.y. population. Thus many of the points that are within Blackwell's generalized <17 m.y. regions are identified by us with older rocks.

The Eastern Mojave Province, much of which has been affected by <17 m.y. igneous activity, has many points closely straddling the Basin and Range (BR) line, but most points (predominantly within the zone of young igneous activity) lie above that line (Figure 10). The range of variation of heat production for the Mojave Block is quite small, and the $q - A_0$ points cluster near the lower end of the BR line. The Mojave Block distribution is very similar to that for the Sonoran Desert, particularly if we exclude the extreme points. Most points for the Mexican Highlands (virtually no igneous activity <17 m.y.) and the Arizona Transition Zone (which had much such activity) fall close to the original BR line, but that curve could not have been defined from either data set. Our conclusion from examining the $q - A_0$ data set is that many factors, including, but not limited to mid-Miocene and younger igneous activity, combine to frustrate a simple interpretation of the $q - A_0$ relation within this study region.

Figures 11–13 revise the discussion of the $q - A_0$ relation for the Basin and Range Province by *Lachenbruch and Sass* [1977]. Figure 11 includes all $q - A_0$ pairs from the Basin and Range Province except for those within and immediately adjacent to active rift zones (the Salton Trough and Rio Grande Rift) and a few isolated sites with heat flow over 200 mW m^{-2}. Figure 12 is a separate histogram for the present study area, which may be compared to the northern Basin and Range (Figure 13). With more than double the number of points for the entire Basin and Range, the distributions are very similar to those described by *Lachenbruch and Sass* [1977] and the mean heat flow, only slightly lower. The shaded outer histograms represent sites within 10 km of mid-Miocene and younger (<17 m.y.) igneous bodies. Overall, these sites do not have higher heat flow than holes drilled in older bodies (the averages shown in parentheses). More importantly, removing the data from late Miocene and younger sites from the total population does not decrease the variance of reduced heat flow (Figures 11b, 12b, and 13b).

Heat Flow and Heat Production in Relation to Metamorphic Core Complexes (MCCs) of the Southern Basin and Range

Some of the most interesting and widely discussed Cenozoic tectonic features of the Mojave-Sonoran region are the metamorphic core complexes (MCCs) shown in black on Figure 5. They represent places where rapid localized extension has been accommodated on upper crustal normal faults to expose a metamorphic "core" of midcrustal rock at the Earth's surface [e.g., *Coney*, 1980; *Spencer and Reynolds*, 1991]. Here we consider their heat flow and radioactive heat production; further discussion is reserved for *Lachenbruch et al.* [this issue]. Most of the MCCs in the mapped region are aligned in a 50- to 100-km-wide band that extends more than 500 km northwesterly across three physiographic subprovinces (the Mexican Highlands, Sonoran Desert, and Eastern Mojave, Figure 5). A conspicuous feature of the heat flow map is a well-defined relative heat flow low (<80 mW m^{-2}) that encloses much of this band. The spacing and local variability of the heat flow measurements do not permit an evaluation of the thermal features of individual MCCs, but it is clear from Figure 5 that most of them have relatively low heat flow. This suggests that the transient warming caused initially by exposure of the midcrust has largely decayed and that the low heat flow might result from the loss of the radioactivity as the upper crust attenuated.

Some evidence for this interpretation can be obtained from the radioactive heat production data summarized in Table 12. The mean heat production from 157 heat flow sites in the southern Basin and Range (2.1 ± .2 μW m^{-3}, ±95% confidence interval) is substantially greater than that (1.3 ± .3 μW m^{-3}) for a comparable number of samples (n = 108) taken for a geochemical study [*Coney and Reynolds*, 1980] in MCCs within the low heat flow band of Figure 5. The latter study was undertaken as part of the National Uranium Resource Evaluation (NURE). Although both samples were limited to fresh crystalline rock (mainly granites, gneisses, mylonites, and schists), and both samples have similar large variability, it is clear from Figure 14 that they represent distinct populations. (They were, however, measured by different methods, but there is no present evidence for a

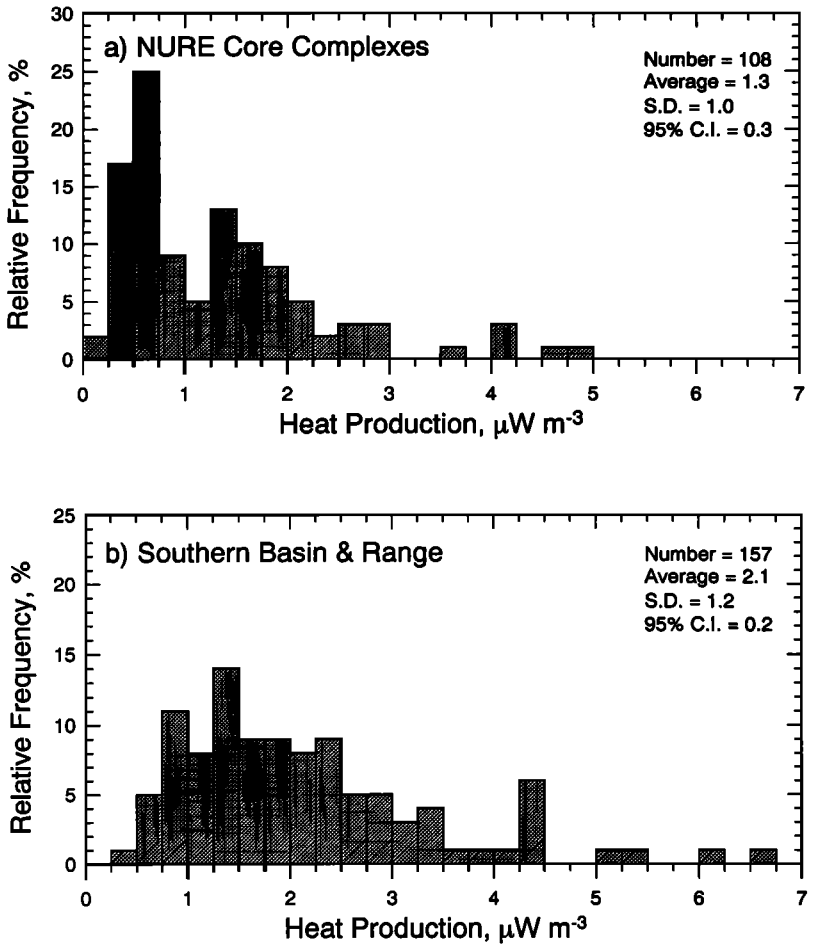

Figure 14. Histograms of radiogenic heat production (a) from NURE samples of metamorphic core complexes in the southern Basin and Range and (b) holes drilled in crystalline rocks, in the southern Basin and Range.

systematic measurement discrepancy.) Table 12 shows that unlike the NURE sample from the MCCs, the mean of samples from the 29 heat flow sites in the low enclosing the MCCs is not significantly below the regional value. Although we do not know structural details at these heat flow sites, few of the boreholes sampled lower plate rocks. Lower plate rocks probably constitute a large fraction of samples in the NURE study, although an attempt to identify lower plate samples and characterize their heat production showed no significant difference from the NURE sample of the MCCs as a whole. In addition, the collection and analysis of six surface samples from the South Mountain MCC showed no significant differences in heat production among lower plate, shear zone, and upper plate rocks at this site, although all measured heat production values at this site were relatively low, consistent with the NURE data.

These somewhat puzzling data might be reconciled by noting that the absence of a relation between heat flow and heat production in the Basin and Range Province implies that heat production does not vary with depth in the upper crust in a simple systematic way, although we know that it must ultimately decrease downward. The heat flow sites are generally composed of typical upper crustal material whereas the NURE sample from the MCCs evidently represents a deeper crustal level, on average showing effects of downward depletion of radioactivity.

A probable explanation for the difference in heat production of samples from the heat flow sites within the heat-flow low (MCCL, Table 12) and the NURE sample is a sampling bias with respect to the MCCs inherent in the selection of heat flow sites. A structural characteristic of the MCCs is the outcrop of lower plate rocks in the higher topography of the ranges in which the MCCs crop out. For a variety of practical and logistical reasons, heat flow sites are usually sited in regions of low topography (see above) in which, paradoxically, outcrops of upper plate rocks are most common. Shallow heat flow holes are not deep enough to penetrate these upper plates, and thus all samples recovered are typically upper plate samples. No such sampling bias is obvious in the NURE data set, and we believe that the NURE data are more regionally representative of the core complex zone for crustal heat production than the heat flow site data. Thus the heat production data are interpreted to support the geologic inference that the MCCs are sites of massive crustal deroofing, and with refined structural estimates of the amount of deroofing at the sample sites, they should contain useful information on the rate of decrease in heat production with depth in the crust. The low heat flow

observed in the vicinity of MCCs is also consistent with extensive deroofing, and it might impose a constraint on their origin, as discussed in the accompanying paper [*Lachenbruch et al.*, this issue].

Summary

We have added sufficiently to the database that existed in 1980 to recharacterize the regional heat flow for the Basin and Range of southern California and Arizona (Figures 3, 4, 5, and 6). With the exception of those regions dominated by hydrologic processes in the upper few hundred meters (primarily the southwestern Colorado Plateau), the observed heat flow patterns can be related to the Cenozoic tectonic history of the region. Zones dominated by compressive tectonics and/or late Cenozoic subduction (e.g., Peninsular Ranges, Transverse Ranges) have heat flows lower than the regional average (60 mW m^{-2} or less). Two elongate zones in which deep crustal rocks are now exposed at the surface are characterized by heat flow less than 80 mW m^{-2}. One zone, extending southeastward from the Transverse Ranges into southwestern Arizona (Figure 5) encompasses most outcrops of the Orocopia Schist, "a late Mesozoic subduction-related terrane" [*Haxel et al.*, 1987]. The other elongate low incorporates the major trend of the metamorphic core complexes [*Coney*, 1980] in central Arizona. Since both features had a deep crustal origin, we conclude that the relatively low heat flow results, at least in part, from relatively low crustal radioactivity associated with tectonic evolution leaving a depleted crustal column.

High heat flows (>80 mW m^{-2}) in the region are generally but not exclusively found in areas of young and contemporary tectonic activity and/or in some of the zones within which Middle Miocene and younger igneous activity is found (Figure 6). A heat flow high associated with the Garlock fault zone is probably the result of Neogene igneous activity, although a minor contribution from frictional heating cannot be ruled out.

Viewed together (Figure 9), there is no simple relation between heat flow and heat production, not surprising in view of the tectonic diversity of the region. When individual tectonic units are considered (Figure 10), some distinct patterns emerge in the heat flow–heat production relation. In particular, there is a tendency for the data from sites located within the <17 m.y. igneous zones to lie on or above the Basin and Range line as originally defined by *Roy et al.* [1968a]. It is not possible, however, to define a statistically valid linear relation for any subprovince, even the Mexican Highlands (Figure 10) within which Middle Miocene and younger volcanism is virtually absent. The complex Cenozoic history of the region, involving lateral movement of tectonic elements, and sources and sinks of varying strength and duration can be invoked to explain the lack of a coherent heat flow–heat production relation.

Appendix: Temperature Data

The temperature data used in the calculation of heat flow were obtained from the last in a time series of temperature profiles as illustrated in Figure A1. To achieve separation of the profiles, the origin of each profile is displaced relative to the preceding one by 1°C. In this example, there are several features common to most of the sites. The first profile,

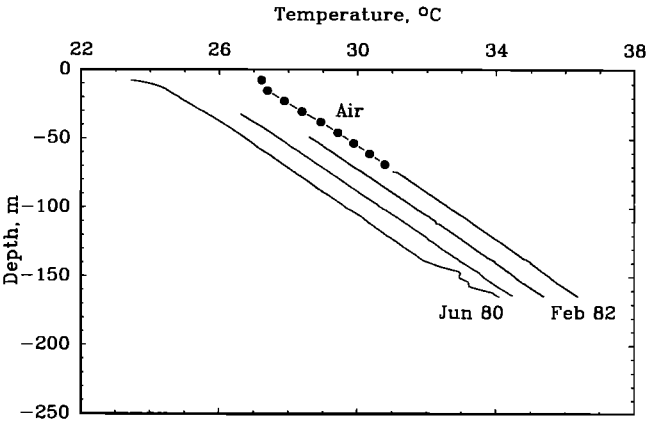

Figure A1. Temperature profiles from a hole in the Mojave Desert. The temperature intercept of each profile is displaced 1°C to the right of the preceding one.

usually obtained a day or two after completion, shows both the effects of circulation of drilling fluid and, in the lowermost 30 m, the heating associated with the curing of the cement in the annulus. Subsequent logs document the decay of these disturbances. The high thermal gradient in the upper 10 m or so of the first profile results from the low thermal conductivity of a thin veneer of sedimentary material. In this

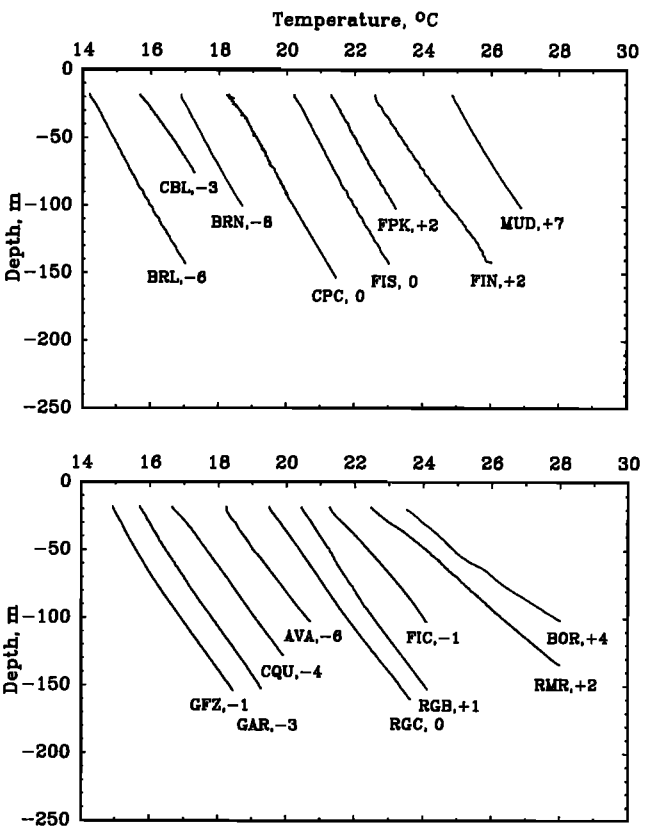

Figure A2. Temperature profiles for the Mojave Block (Figure 3 and Table 3). Temperature origins are displaced by the number of degrees shown to the right of the well designation. Profiles not shown are published by *Sass et al.* [1986], *Lachenbruch and Sass* [1988], or *Sass et al.* [1992].

instance, as in perhaps 10% of completions, there was a leaky coupling somewhere in the casing string as evidenced by a slow decline in the water level in the casing. The continuous profile in the lower part of the well was supplemented in the final log by discrete measurements in air (equilibration time in air is tens of minutes as opposed to a few seconds in water).

Temperature profiles used in the heat flow calculations of Tables 3–8 are grouped in Figures A2–A8. All profiles have the same aspect ratio such that 1°C on the temperature scale is equivalent to 25 m depth. For this ratio, a line inclined at 45°C to the vertical is equivalent to 40°C km^{-1}. Thermal conductivity profiles are not graphed, because in the great majority of cases, no depth relation can be discerned amid the scatter (typically ±20%) in individual conductivity values.

As stated in the body of the text, there is very little indication of vertical fluid movement in the temperature profiles. The only conspicuous exception is RSS (Figure A4)

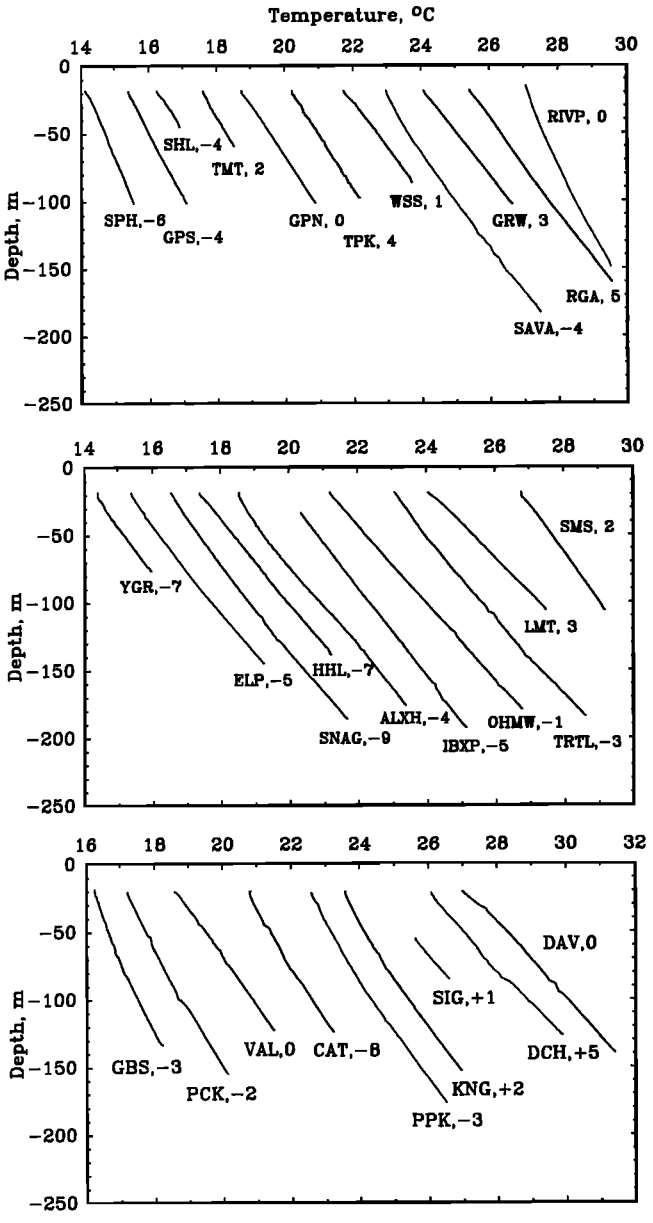

Figure A3. Temperature profiles for the Eastern Mojave Province, California, Arizona, and Nevada (Figures 3 and 4 and Table 4). Temperature origins are displaced by the number of degrees shown to the right of the well designation.

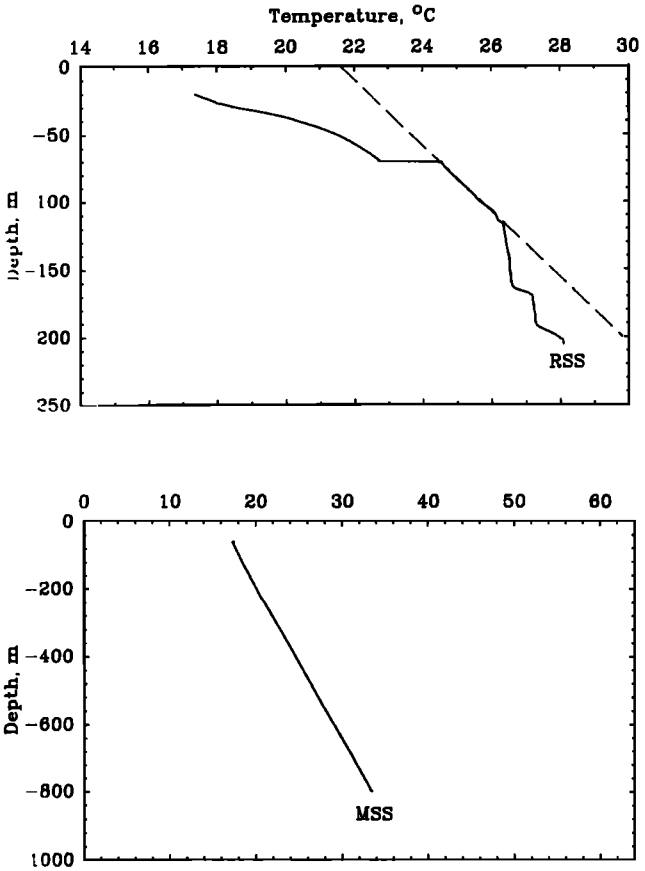

Figure A4. Temperature profiles for deeper wells of the Eastern Mojave Province. RSS is a cased water well having many slotted intervals. Interpreted equilibrium profile is indicated by dashed line (Figure 3 and Table 4).

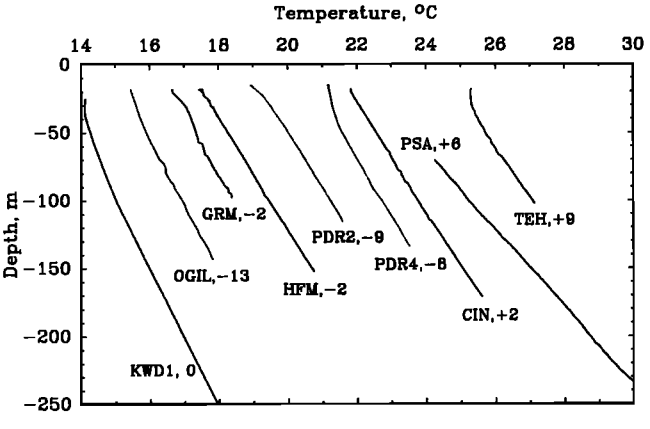

Figure A5. Temperature profiles from the Salton Trough, Peninsular Ranges, Transverse Ranges, and Tehachapi Mountains (Figure 3 and Table 5). Temperature origins are displaced by the number of degrees shown to the right of the well designation.

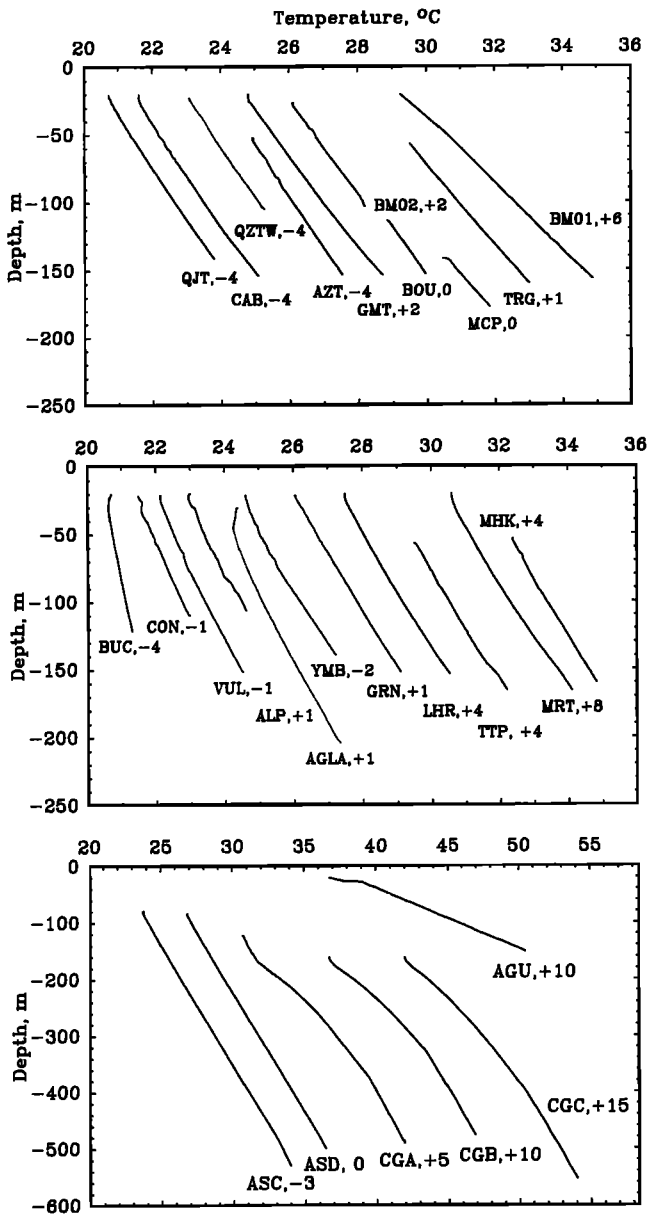

Figure A6. Temperature profiles from the Sonoran Desert Region, Arizona Basin and Range (Figure 4 and Table 6). Temperature origins are displaced by the number of degrees shown to the right of the well designation.

which was an unused water well with slotted casing. Despite the evidence for vertical and lateral water movement in that well, we are reasonably confident that the linear segment chosen for the heat flow represents undisturbed formation temperature. In particular, the surface intercept of about 21.5°C (dashed line, Figure A4) is reasonable for that altitude and latitude.

Figure A6 contains two extreme profiles, both of which are probably affected by fluid movement. BUC was drilled in an attempt to provide confirmation for the high heat flow values obtained by *Warren et al.* [1969] at Buckeye Hills and Rainbow Valley. In the latter well (UCSD-2) a nearly isothermal condition was observed from the water table at a depth of 100+ m to total depth of 250 m. In the intervening decade, a dam was built in the area, and the water table rose considerably with some flooding of nearby fields (S. J. Reynolds, personal communication, 1990). BUC, located about 3.7 km NW of UCSD-1 [*Warren et al.*, 1969] encountered water at 64 m and drilling was discontinued at 122 m because of drilling problems associated with entry of water. The gradient of 7.9°C km^{-1} was by far the lowest encountered in the Basin and Range portion of this study. We chose to violate this point when contouring (Figures 5 and 6) because of the evidence for lateral hydrologic flow in the formation.

AGU (Figure A6) which provided the highest gradient and heat flow outside of the Salton Trough, was drilled in a very arid area having no local surface evidence of hydrothermal

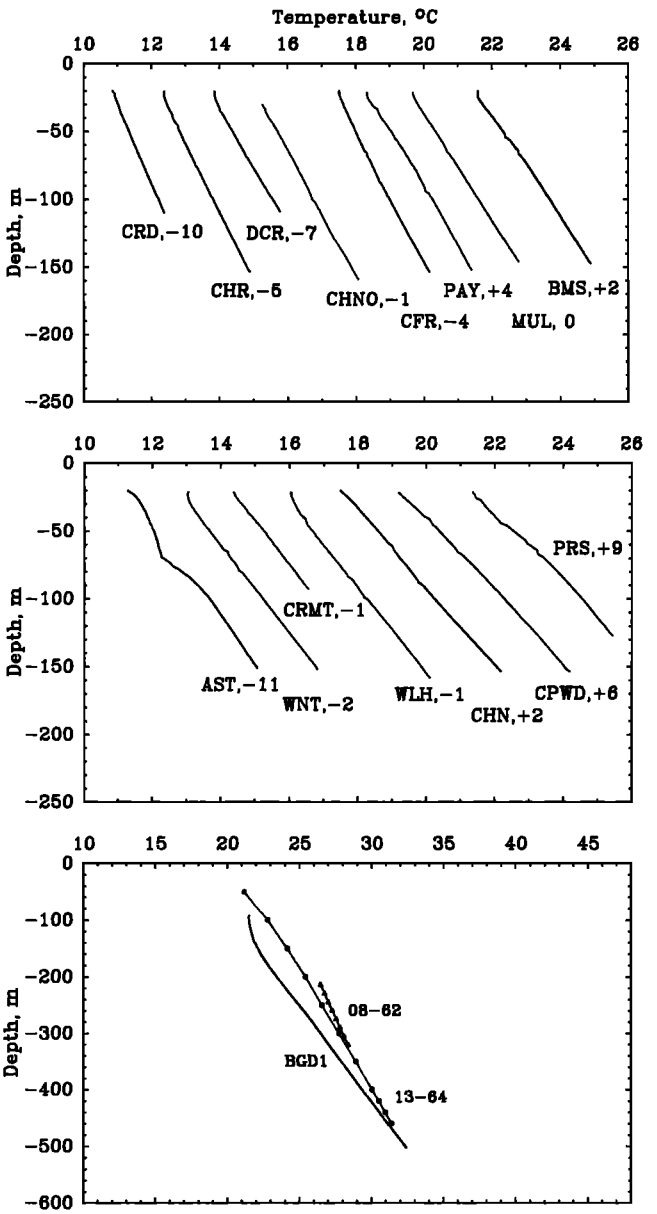

Figure A7. Temperature profiles from the Arizona Transition Zone (Figure 4 and Table 7). Temperature origins are displaced by the number of degrees shown to the right of the well designation. The profile for BGD1 was obtained in the Bagdad open pit. Nearby profiles [*Roy et al.*, 1968b; *Decker and Roy*, 1974] are shown for comparison.

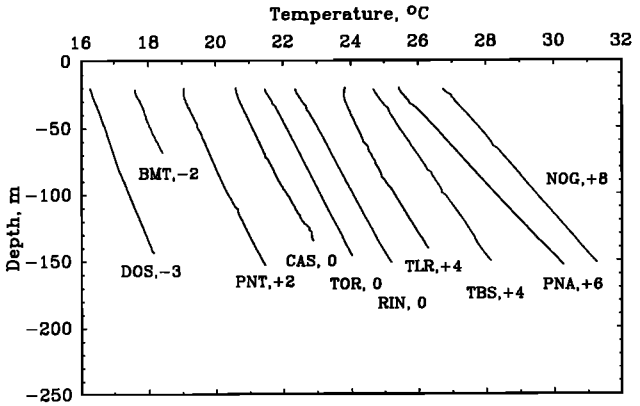

Figure A8. Temperature profiles from the Mexican Highlands, Arizona Basin and Range (Figure 4 and Table 8). Temperature origins are displaced by the number of degrees shown to the right of the well designation.

activity. The high heat flow at AGU probably reflects the proximity of the site to either the nearby Quitaboquito hot spring or the Pliocene-Pleistocene Pinacate Volcanic Field, just to the south in Sonora, Mexico [*Shafiquallah et al.*, 1978].

Our reoccupation of the Bagdad, Arizona, site is of historial interest where *Roy et al.* [1968a] found a significantly lower heat flow there than that predicted by their Basin and Range line. They theorized that because the granite stocks from which the $q - A_0$ pairs were derived were small and surrounded by rocks of much lower radioactivity, that a three-dimensional adjustment for horizontal heat loss was needed; they made such an adjustment (about 8 mW m^{-2}) to their measured heat flow (see Table 2 and Figure 5 of *Roy et al.* [1968a]). Our heat flow point (BGD1) was in the open pit of the Bagdad mine, within a large stock of granite. The temperature profile (Figure A7) contrasts markedly with those obtained by *Roy et al.* [1968b] and provides a heat flow somewhat higher than even their corrected value (82 versus 77 mW m^{-2}). In fact, our $q - A_0$ pair of 82 mW m^{-2} and 2.5 μW m^{-3} (Table 7) plots very close to the Basin and Range line defined by *Roy et al.* [1968a]. It is unclear from the available data whether lateral heat flow was the principal reason for the low value obtained by *Roy et al.* [1968a, b] or whether other sources of scatter (as discussed by *Sass et al.* [1971b]) played a role.

Acknowledgments. Although the majority of the heat flow holes were drilled prior to the official inception of the U.S. Continental Scientific Drilling Program (USCSDP), this heat flow drilling program should probably be counted as a significant contribution to the total USCSDP effort. Alan R. Smith (Lawrence Berkeley National Laboratory) performed most of the determinations of radioactive element abundances. We thank David Blackwell, Rick Blakely, Warren Hamilton, Gordon Haxel, Keith Howard, Jill McCarthy, Rick Saltus, and Mary Lou Zoback for reviews of an earlier draft. We are grateful to Fred Grubb, Robert Husk, Jack Kennelly, Jackson Porter, Eugene Smith, Walter Wendt, John Ziagos, and Mary Lou Zoback for technical contributions. We also thank JGR reviewers William Gosnald, Dale Issler, and Leigh Royden for their constructive comments.

References

Appel, C. L., and D. J. Bills, Map showing ground-water conditions in the Canyon Diablo area, Coconino and Navajo Counties, Arizona—1979, scale 1:125,000, *U.S. Geol. Surv. Water Resour. Invest. Open File Rep., 80–747*, 1980.

Appel, C. L., and D. J. Bills, Maps showing ground-water conditions in the San Francisco Peaks Area, Coconino County, Arizona—1979, scale 1:125,000, *U.S. Geol. Surv. Water Resour. Invest. Open File Rep., 81–914*, 1981.

Aydin, A., and A. Nur, Evolution of pull-apart basins and their scale independence, *Tectonics, 1*, 91–105, 1982.

Beck, A. E., Methods for determining thermal conductivity and thermal diffusivity, in *Handbook of Terrestrial Heat-Flow Density Determination*, edited by R. Haenel, L. Rybach, and L. Stegena, pp. 87–124, Kluwer Academic, Norwell, Mass., 1988.

Beck, A. E., and N. Balling, Determination of Virgin Rock Temperatures, in *Handbook of Terrestrial Heat-Flow Density Determination*, edited by R. Haenel, L. Rybach, and L. Stegena, pp. 59–85. Kluwer Academic, Norwell, Mass., 1988.

Birch, F. Flow of heat in the Front Range, Colorado, *Geol. Soc. Am. Bull., 61*, 567–630, 1950.

Birch, F., R. F. Roy, and E. R. Decker, Heat flow and thermal history in New England and New York, in *Studies of Appalachian Geology: Northern and Maritime*, edited by E-an Zen, W. S. White, J. B. Hadley, and J. B. Thompson Jr., pp. 437–151, Wiley-Interscience, New York, 1968.

Blackwell, D. D., Heat-flow determinations in the northwestern United States, *J. Geophys. Res., 74*, 992–1007, 1969.

Blackwell, D. D., Heat flow and energy loss in the western U.S., in Cenozoic Tectonics and Regional Geophysics of the Western Cordillera, edited by R. B. Smith and G. P. Eaton, *Mem. Geol. Soc. Am., 152*, 175–208, 1978.

Blackwell, D. D., and R. E. Spafford, Experimental methods in continental heat flow, in *Experimental Methods in Physics*, vol. 24, *Geophysics, Part B, Field Measurements*, edited by C. G. Sarmus and T. L. Henyey, pp. 189–226, Academic, San Diego, Calif., 1987.

Blackwell, D. D., and J. L. Steele, Geothermal map of North America, *DNAG Neotectonic Series*, scale 1:5,000,000, *Map CSM-007, 4 sheets, Geol. Soc. of Am., Boulder, Colo., 1992.*

Blackwell, D. D., J. L. Steele, and L. S. Carter, Heat-flow patterns of the North American continent: A discussion of the geothermal map of North America, in *Neotectonics of North America*, vol. 1, edited by D. B. Slemmons, E. R. Engdahl, M. D. Zoback, and D. D. Blackwell, pp. 423–436, Geological Society of America, Boulder, Colo., 1991.

Bredehoeft, J. D., and I. S. Papadopoulos, Rates of vertical groundwater movement estimated from the earth's thermal profile, *Water Resour. Res., 1*, 325–328, 1965.

Byerly, P. E., and R. H. Stolt, An attempt to define the Curie point isotherm in northern and central Arizona, *Geophysics, 42*, 1394–1400, 1977.

Clark, M. M., Map showing recently active breaks along the Garlock and associated faults, California, scale 1:24,000, *U.S. Geol. Surv. Misc. Geol. Invest. Map, I-741*, 1973.

Combs, J., Heat flow determinations in the Coso Geothermal Area, California, *Coso Geotherm. Proj. Tech. Rep. 3*, Energy Res. and Dev. Admin., Germantown, Md., 1976.

Coney, P. J., Cordilleran metamorphic core complexes: An overview, in Cordilleran Metamorphic Core Complexes, edited by M. D. Crittenden, Jr., P. J. Coney, and G. H. Davis, *Mem. Geol. Soc. Am., 153*, 7–31, 1980.

Coney, P. J., and T. A. Harms, Cordilleran metamorphic core complexes: Cenozoic extensional relics of Mesozoic compression, *Geology, 12*, 550–554, 1984.

Coney, P. J., and S. J. Reynolds, Cordilleran metamorphic core complexes and their uranium favorability, final report, Geosci. Dep., Univ. of Ariz., Tucson, 1980.

Cooley, M. E., Spring flow from Pre-Pennsylvanian rocks in the southwestern part of the Navajo Indian Reservation, Arizona, *U.S. Geol. Surv. Prof. Pap., 521-F*, 15 pp., 1976.

Cooley, M. E., J. W. Harshbarger, J. P. Akers, and W. F. Hardt, Regional hydrogeology of the Navajo and Hopi Indian Reservations, Arizona, New Mexico and Utah, with a section on vegetation by O. N. Hicks, *U.S. Geol. Surv. Prof. Pap., 521-A*, 61 pp., 1969.

Decker, E. R., and R. F. Roy, Basic heat-flow data from the Eastern and Western United States, in *Basic Heat-Flow Data from the United States*, compiled by J. H. Sass and R. J. Munroe, *U.S. Geol. Surv. Open File Rep., 74-9*, 7-6–7-90, 1974.

Decker, E. R., H. P. Heasler, K. L. Buelow, K. H. Baker, and J. S. Hallin, Significance of past and recent heat flow and radioactivity studies in the Southern Rocky Mountains region, *Geol. Soc. Am. Bull., 100*, 1851–1885, 1988.

De Rito, R. F., A. H. Lachenbruch, T. H. Moses Jr., and R. J. Munroe, Heat flow and thermotectonic problems of the central Ventura Basin, southern California, *J. Geophys. Res., 94*, 681–699, 1989.

Dillon, J. T., G. B. Haxel, and R. M. Tosdal, Structural evidence for northeastward movement on the Chocolate Mountains thrust, southeasternmost California, *J. Geophys. Res., 95*, 19,953–19,971, 1990.

Dokka, R. K., Displacements on late Cenozoic strike-slip faults of the central Mojave Desert, California, *Geology, 11*, 305–308, 1983.

Dokka, R. K., The Mojave extensional belt of southern California *Tectonics, 8*, 363–390, 1989.

Gans, P. B., G. A. Mahood, and E. Schermer, Synextensional magmatism in the Basin and Range province: A case study from the eastern Great Basin, *Spec. Pap. Geol. Soc. Am., 233*, 53 pp., 1989.

Garfunkel, Z., Model for the Late Cenozoic tectonic history of the Mojave Desert, California, and for its relation to adjacent regions, *Geol. Soc. Am. Bull., 85*, 1931–1944, 1974.

Haxel, G. B., J. R. Budahn, T. L. Fries, B.-S. W. King, L. D. White, and P. J. Aruscavage, Geochemistry of the Orocopia Schist, southeastern California: Summary, *Ariz. Geol. Soc. Dig., 18*, 49–64, 1987.

Henyey, T. L., Heat flow near major strike-slip faults in central and southern California, Ph.D. thesis, Calif. Inst. of Technol., Pasadena, 1968.

Henyey, T. L., and G. J. Wasserburg, Heat flow near major strike-slip faults in California, *J. Geophys. Res., 76*, 7924–7946, 1971.

Hong, M. R., C. L. V. Aiken, and W. J. Peeples, Aeromagnetic anomaly and analysis of the depth-to-Curie isotherm, *Soc. Explor. Geophys. Annu. Meet. Tech. Program Abstr. Biograph., 51*, 11–12, 1981.

Howard, K. A., R. W. Simpson, and G. B. Haxel, Introduction to special section on the California-Arizona crustal transect: Part 1, *J. Geophys. Res., 95*, 461–462, 1990.

Huntoon, P. W., Fault controlled ground-water circulation under the Colorado River, Marble Canyon, Arizona, *Ground Water, 19*, 20–27, 1981.

Jaeger, J. C., and J. H. Sass, Lees's topographic correction in heat flow and the geothermal flux in Tasmania, *Geofis. Pura Appl., 54*, 53–63, 1963.

Johnson, P. W., and R. B. Sanderson, Spring flow into the Colorado River, Lees Ferry to Lake Mead, Arizona, *Water Resour. Rep. 34*, 26 pp., Ariz. State Land Dep., Phoenix, Ariz., 1968.

Lachenbruch, A. H., Preliminary geothermal model of the Sierra Nevada, *J. Geophys. Res., 73*, 6977–6989, 1968a.

Lachenbruch, A. H., Rapid estimation of the topographic disturbance to superficial thermal gradients, *Rev. Geophys., 6*, 365–400, 1968b.

Lachenbruch, A. H., Crustal temperature and heat production: Implications of the linear heat flow relation, *J. Geophys. Res., 75*, 3291–3300, 1970.

Lachenbruch, A. H., and C. M. Bunker, Vertical gradients of heat production in the continental crust, 2, Some estimates from borehole data: *J. Geophys. Res., 76*, 3852–3860, 1971.

Lachenbruch, A. H., and J. H. Sass, Thermo-mechanical aspects of the San Andreas fault system, in Proceedings of the Conference on the Tectonic Problems of the San Andreas Fault System, edited by R. L. Kovach and A. Nur, *Stanford Univ. Publ. Geol. Sci., 13*, 192–205, 1973.

Lachenbruch, A. H., and J. H. Sass, Heat flow in the United States and the thermal regime of the crust, in *The Earth's Crust, Geophys. Monogr. Ser.*, vol. 20, edited by J. G. Heacock, pp. 626–675, AGU, Washington, D.C., 1977.

Lachenbruch, A. H., and J. H. Sass, Models of an extending lithosphere and heat flow in the Basin and Range province, *Mem. Geol. Soc. Am., 152*, 209–250, 1978.

Lachenbruch, A. H., and J. H. Sass, Heat flow and energetics of the San Andreas fault zone, *J. Geophys. Res., 85*, 6185–6223, 1980. (Corrections to "Heat flow and energetics of the San Andreas fault zone" and some additional comments on the relation between fault friction and observed heat flow, *J. Geophys. Res., 86*, 7171–7172, 1981.)

Lachenbruch, A. H., and J. H. Sass, The stress heat-flow paradox and thermal results from Cajon Pass, *Geophys. Res. Lett., 15*, 981–984, 1988.

Lachenbruch, A. H., and J. H. Sass, Heat flow from Cajon Pass, fault strength, and tectonic implications, *J. Geophys. Res., 97*, 4995–5015, 1992. (Correction to "Heat flow from Cajon Pass, fault strength, and tectonic implications," *J. Geophys. Res., 97*, 17,711, 1992.)

Lachenbruch, A. H., J. H. Sass, and S. P. Galanis, Jr., New heat-flow results from southern California (abstract), *Eos Trans. AGU, 59*, 1051, 1978.

Lachenbruch, A. H., J. H. Sass, and S. P. Galanis Jr., Heat flow in southernmost California and the origin of the Salton Trough *J. Geophys. Res., 90*, 6709–6736, 1985.

Lachenbruch, A. H., J. H. Sass, T. H. Moses Jr., and S. P. Galanis Jr., Thermal studies at the Cajon Pass borehole (abstract), *Eos Trans. AGU, 67*, 379–380, 1986a.

Lachenbruch, A. H., J. H. Sass, T. H. Moses Jr., and S. P. Galanis Jr., Thermal considerations and the Cajon Pass borehole, *U.S. Geol. Surv. Open File Rep., 86-469*, 1986b.

Lachenbruch, A. H., J. H. Sass, and P. Morgan, Thermal regime of the southern Basin and Range province, 2, Implications of heat flow for regional extension and metamorphic core complexes, *J. Geophys. Res.*, this issue.

Lee, T. C., Heat flow through the San Jacinto fault zone, southern California. *Geophys. J. R. Astron. Soc., 54*, 721–731, 1983.

Levings, G. W., and L. J. Mann, Maps showing ground-water conditions in the upper Verde River area, Yavapai and Coconino Counties, Arizona—1978, scale, 1:125,000, *U.S. Geol. Surv. Water Resour. Invest. Open File Rep., 80-726*, 1980.

Mayer, L., Topographic constraints on models of lithospheric stretching of the Basin and Range province, western United States, in Extensional Tectonics of the Southwestern United States: A Perspective on Processes and Kinematics, edited by L. Mayer, *Spec. Pap. Geol. Soc. Am., 208*, 1–14, 1986.

Morgan, P., and W. D. Gosnold, Heat flow and thermal regimes in the continental United States, in Geophysical Framework of the Continental United States, edited by L. C. Pakiser and W. D. Mooney, *Mem. Geol. Soc. Am., 172*, 493–522, 1989.

Moses, T. H., Jr., and J. H. Sass, Drilling techniques presently in use by the Geothermal Studies Project, *U.S. Geol. Surv. Open File Rep., 79-763*, 1979.

Newmark, R. L., P. W. Kasameyer, and L. W. Younker, Shallow drilling in the Salton Sea region: The thermal anomaly, *J. Geophys. Res., 93*, 13,005–13,024, 1988.

Powell, W. G., D. S. Chapman, N. Balling, and A. E. Beck, Continental heat-flow density, in *Handbook of Terrestrial Heat Flow Density Determinations*, edited by R. Haenel, L. Rybach, and L. Stegena, pp. 167–222, Kluwer Academic, Norwell, Mass., 1988.

Reynolds, S. J., F. P. Florence, J. W. Welty, M. S. Roddy, D. A. Currier, A. V. Anderson, and S. B. Keith, Compilation of radiometric age determinations in Arizona, *Ariz. Geol. Surv. Bull., 197*, 258 pp., 1986.

Roy, R. F., D. D. Blackwell, and F. Birch, Heat generation of plutonic rocks and continental heat-flow provinces, *Earth Planet. Sci. Lett., 5*, 1–12, 1968a.

Roy, R. F., E. R. Decker, D. D. Blackwell, and F. Birch, Heat flow in the United States. *J. Geophys. Res., 73*, 5207–5221, 1968b.

Roy, R. F., D. D. Blackwell, and E. R. Decker, Continental heat flow, in *The Nature of the Solid Earth*, edited by E. C. Robertson, pp. 506–543, McGraw-Hill, New York, 1972.

Rybach, L., Determination of heat production rate, in *Handbook of Terrestrial Heat-Flow Density Determination*, edited by R. Haenel, L. Rybach, and L. Stegena, pp. 125–142, Kluwer Academic, Norwell, Mass., 1988.

Saltus, R. W., and A. H. Lachenbruch, Thermal evolution of the

Sierra Nevada: Tectonic implications of new heat flow data, *Tectonics*, *10*, 325–344, 1991.

Saltus, R. W., A. H. Lachenbruch, S. P. Galanis Jr., and J. H. Sass, Heat flow in the southern Sierra Nevada, California (abstract), *Eos Trans. AGU*, *69*, 1450, 1988.

Sass, J. H., and A. H. Lachenbruch, Heat-flow field of the California-Arizona crustal experiment and adjacent areas (abstract), *Geol. Soc. Am. Abstr. Programs*, *19*, 829, 1987.

Sass, J. H., A. H. Lachenbruch, and R. J. Munroe, Thermal conductivity of rocks from measurements on fragments and its application to heat flow determinations. *J. Geophys. Res.*, *76*, 3391–3401, 1971a.

Sass, J. H., A. H. Lachenbruch, R. J. Munroe, G. W. Greene, and T. H. Moses Jr., Heat flow in the western United States, *J. Geophys. Res.*, *76*, 6376–6413, 1971b.

Sass, J. H., D. D. Blackwell, D. S. Chapman, J. K. Costain, E. R. Decker, L. A. Lawver, and C. A. Swanberg, Heat flow from the crust of the United States, in *Physical Properties of Rocks and Minerals*, edited by Y. S. Touloukian, W. R. Judd, and R. F. Roy, pp. 503–548, McGraw-Hill, New York, 1981a.

Sass, J. H., R. J. Munroe, and Claudia Stone, Heat flow from five uranium test wells in West-Central Arizona, *U.S. Geol. Surv. Open File Rep.*, *81–1089*, 42 pp., 1981b.

Sass, J. H., Claudia Stone, and D. J. Bills, Shallow subsurface temperatures and some estimates of heat flow from the Colorado Plateau of northeastern Arizona, *U.S. Geol. Surv. Open File Rep.*, *82–994*, 112 pp., 1982.

Sass, J. H., S. P. Galanis, Jr., A. H. Lachenbruch, B. V. Marshall, and R. J. Munroe, Temperature, thermal conductivity, heat flow, and radiogenic heat production from unconsolidated sediments of the Imperial Valley, California, *U.S. Geol. Surv. Open File Rep.*, *84–490*, 37 pp., 1984a.

Sass, J. H., J. P. Kennelly Jr., E. P. Smith, and W. E. Wendt, Laboratory line-source methods for the measurement of thermal conductivity of rocks near room temperature, *U.S. Geol. Surv. Open File Rep.*, *84–91*, 1984b.

Sass, J. H., Claudia Stone, and R. J. Munroe, Thermal conductivity determinations on solid rock—A comparison between a steady-state divided-bar apparatus and a commercial transient line-source device, *J. Volcanol. Geotherm. Res.*, *20*, 145–153, 1984c.

Sass, J. H., A. H. Lachenbruch, S. P. Galanis Jr., R. J. Munroe, and T. H. Moses Jr., An analysis of thermal data from the vicinity of Cajon Pass, California, *U.S. Geol. Surv. Open File Rep.*, *86–468*, 1986.

Sass, J. H., G. B. Haxel, and Ivo Lucchita, CACTIS Meeting examines crustal transect, *Ariz. Geol.*, *18*, 7, 1988a.

Sass, J. H., S. S. Priest, L. E. Duda, C. C. Carson, J. D. Hendricks, and L. C. Robison, Thermal regime of the State 2-14 well, Salton Sea Scientific Drilling Project, *J. Geophys. Res.*, *93*, 12,995–13,004, 1988b.

Sass, J. H., A. H. Lachenbruch, T. H. Moses Jr., and P. Morgan, Heat flow from a scientific research well at Cajon Pass, California, *J. Geophys. Res.*, *97*, 5017–5030, 1992.

Shafiquallah, M., P. E. Damon, D. J. Lynch, P. H. Kuck, and W. A. Rehrig, Mid-Tertiary magmatism in southeastern Arizona, in Land of Cochise, edited by J. F. Callender et al., *Field Conf. Guideb. N. M. Geol. Soc.*, *29th*, 231–241, 1978.

Shearer, C., and M. Reiter, Terrestrial heat flow in Arizona, *J. Geophys. Res.*, *86*, 6249–6260, 1981.

Smiley, T. L., The geology and dating of Sunset Crater, Flagstaff, Arizona, in Black Mesa Basin, Northeast Arizona, *Field Conf. Guideb. N. M. Geol. Soc.*, *9th*, 186–190, 1958.

Smith, R. B., Seismicity, crustal structure, and intraplate tectonics of the interior of the western Cordillera, in Cenozoic Tectonics and Regional Geophysics of the Western Cordillera, edited by R. B. Smith and G. P. Eaton, *Mem. Geol. Soc. Am.*, *152*, 111–144, 1978.

Spencer, J. E., and S. J. Reynolds, Tectonics of mid-Tertiary extension along a transect through west central Arizona, *Tectonics*, *10*, 1204–1221, 1991.

Stauber, D. A., Two-dimensional compressional wave velocity structure under San Francisco volcanic field, Arizona, from teleseismic *P* residual measurements, *J. Geophys. Res.*, *87*, 5451–5459, 1982.

Stewart, J. H., and J. E. Carlson, Generalized maps showing distribution, lithology, and age of Cenozoic igneous rocks in the western United States, in Cenozoic Tectonics and Regional Geophysics of the Western Cordillera, edited by R. B. Smith and G. P. Eaton, *Mem. Geol. Soc. Am.*, *152*, 263–264, 1978.

Swanberg, C. A., and P. Morgan, The silica heat flow interpretation technique: Assumptions and applications, *J. Geophys. Res.*, *85*, 7206–7214, 1980.

Warren, R. E., J. G. Sclater, V. Vacquier, and R. F. Roy, A comparison of terrestrial heat flow and transient geomagnetic fluctuations in the southwestern United States, *Geophysics*, *34*, 463–478, 1969.

Wollenberg, H. A., Radiometric methods, in *Nuclear Methods in Mineral Exploration*, pp. 5–36, Elsevier, New York, 1977.

S. P. Galanis Jr., A. H. Lachenbruch, T. H. Moses Jr., and R. J. Munroe, U.S. Geological Survey, 345 Middlefield Road, MS 977, Menlo Park, CA 94025. (e-mail: pgalanis@isdmnl.wr.usgs.gov; alachenbruch@isdmnl.wr.usgs.gov; tmoses@hq.wr.usgs.gov)

P. Morgan, Department of Geology, Northern Arizona University, P.O. Box 6030, Flagstaff, AZ 86011. (e-mail: morgan@unkar.glg.nau.edu)

S. S. Priest and J. H. Sass, U.S. Geological Survey, 2255 North Gemini Dr., Flagstaff, AZ 86001. (e-mail: jsass@aa.wr.usgs.gov)

(Received March 4, 1994; revised July 11, 1994;
accepted July 18, 1994.)